Ferroelectric Hf 0.5 Zr 0.5 O 2 films with improved endurance obtained through low temperature epitaxial growth on seed layers

Tingfeng Song, Romain Bachelet, Guillaume Saint-Girons, Ignasi Fina, Florencio Sánchez

Nanoscale

Ferroelectric $Hf_{0.5}Zr_{0.5}O_2$ films with improved endurance by low temperature epitaxial growth on seed layers

Journal:	*Nanoscale*
Manuscript ID	NR-ART-10-2022-005935.R1
Article Type:	Paper
Date Submitted by the Author:	n/a
Complete List of Authors:	Song, Tingfeng; Institut de Ciència de Materials de Barcelona (ICMAB-CSIC) Bachelet, Romain; Ecole Centrale de Lyon, Nanotechnolies Saint-Girons, Guillaume; CNRS, Fina, Ignasi; Consejo Superior de Investigaciones Cientificas, Magnetic Materials and Functional Oxides Sanchez, Florencio; Institut de Ciencia de Materials de Barcelona (ICMAB-CSIC),

Nanoscale

Guidelines for Referees

Thank you very much for agreeing to review this manuscript for *Nanoscale*.

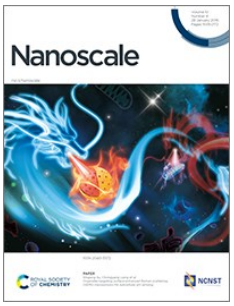

Nanoscale is a high impact international journal, publishing high quality research across nanoscience and nanotechnology. It publishes a full mix of research articles on experimental and theoretical work, including reviews, communications and full papers.

Nanoscale Associate Editors stress very high standards for acceptance in the journal. Articles must report extremely novel, very high quality, reproducible new work of broad general interest.

Nanoscale's Impact Factor is **8.307** (2021 Journal Citation Reports®)

The following manuscript has been submitted for consideration as a

PAPER

For acceptance, papers must report original scientific work that has not been published previously. Full papers do not have a page limit and should be appropriate in length for scientific content.

When preparing your report, please:

- Focus on the **originality**, **importance**, **impact** and **reproducibility** of the science.
- Refer to the **journal scope and expectations**.
- **State clearly** whether you think the article should be accepted or rejected and give detailed comments (with references) both to help the Editor to make a decision on the paper and the authors to improve it
- **Inform the Editor** if there is a conflict of interest, a significant part of the work you cannot review with confidence or if parts of the work have previously been published.
- **Provide your report rapidly** or inform the Editor if you are unable to do so.

Best regards,

Professor Chunli Bai
Editor-in-Chief, *Nanoscale*

Professor Dirk Guldi
Editor-in-Chief, *Nanoscale*

Dr Heather Montgomery
Managing Editor, *Nanoscale*

Contact us

Please visit our reviewer hub for further details of our processes, policies and reviewer responsibilities as well as guidance on how to review, or click the links below.

What to do when you review

Reviewer responsibilities

Process & policies

A seed layer of thickness about 2 nm allows reducing in the threshold temperature for epitaxy of $Hf_{0.5}Zr_{0.5}O_2$ films in at least 200 °C. Films deposited at low temperature on seed layers show reduced ferroelectric fatigue and improved endurance.

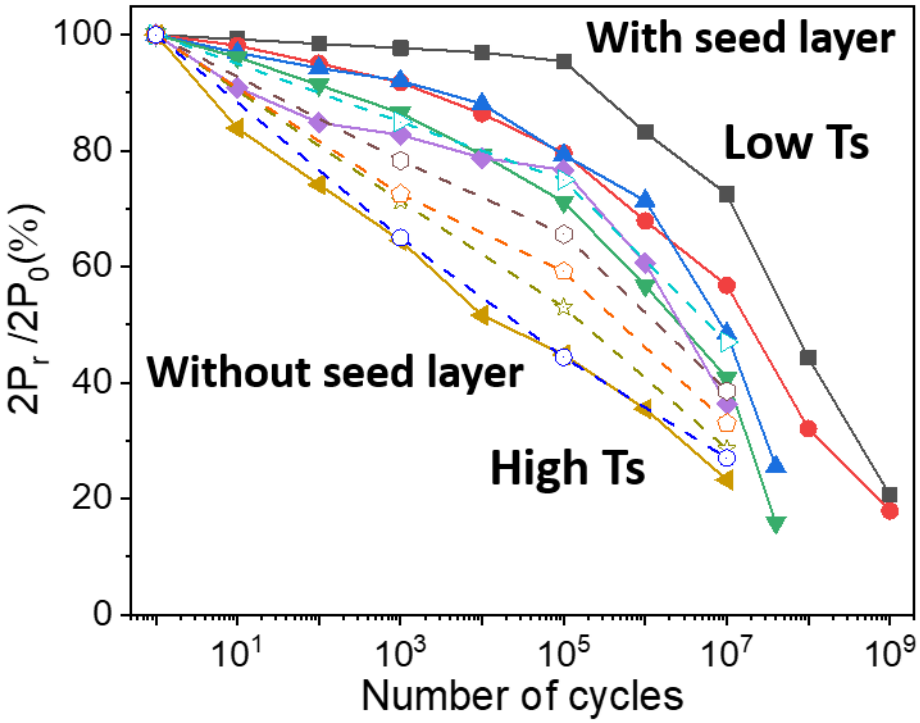

Barcelona, December 29, 2022

Dear editor,

We thank the referees for the careful reading of our revised manuscript, and for their constructive comments. Below we indicate point by point all comments of the referees and the changes introduced in the revised version of the manuscript.

Reply to Referee 1.

Referee #1: "In the manuscript "Low temperature epitaxial growth of ferroelectric Hf0.5Zr0.5O2 films on seed layers", Song et al. demonstrated how a seed layer can be used to reduce the growth temperature of the epitaxial film which can exhibit reduced fatigue. They studied three series of samples: (1) HZO on Si (2) HZO (without a seed layer) on STO/LSMO (3) HZO (with HZO seed layer) on STO/LSMO. This HZO seed layer is grown at 800°C. The experimental results were compared between these three series of samples.

The work is systematic and the topic can be interesting to the readers. However, the following facts must be addressed."

Response: Thanks for the detailed review and the comments. We have revised the manuscript accordingly.

1: "In my opinion, one of the most important observations in this work is improved endurance / reduced fatigue. This can be highlighted in the title too."

Response: The referee is right. This important result was not indicated in the title. We have changed it.

Revised version: The title "Low temperature epitaxial growth of ferroelectric $Hf_{0.5}Zr_{0.5}O_2$ films on seed layers" has been replaced by "Ferroelectric $Hf_{0.5}Zr_{0.5}O_2$ films with improved endurance by low temperature epitaxial growth on seed layers".

2: "It is hard to understand the topic from the abstract. In the abstract, the aim of the work appears to be low temperature growth of HZO. However, the results show the motivation as a better ferroelectric performance (no wakeup, improved endurance and reduced fatigue) of the films"

Response: We have modified the abstract, emphasizing the improvement of the polarization behavior against cycling in low-T_S films grown on seed layers.

Revised version: In the abstract "Epitaxial films grown at 550 °C have high polarization with no wake-up effect and show greatly reduced fatigue." has been replaced by "The threshold temperature for epitaxy is reduced from about 750 °C to about 550 °C by using a seed layer. Epitaxial films deposited at low temperature exhibit highly enhanced endurance, and films grown at 550 - 600 °C have high polarization, no wake-up effect, and greatly reduced fatigue and improved endurance in comparison with the films deposited at high temperature without a seed layer."

3: "[Introduction] "*Doped HfO2 films exhibit robust ferroelectricity at room temperature,…*". Ferroelectricity is observed in undoped HfO2 films also. (a) Appl. Phys. Lett. 106, 232905 (2015); https://doi.org/10.1063/1.4922272 (b) Appl. Phys. Lett. 110, 022903 (2017); https://doi.org/10.1063/1.4973928 (c) Adv. Mater. Interfaces 2019, 1900042; https://doi.org/10.1002/admi.201900042"

Response: We have rephrased slightly the first paragraph of Introduction

Revised version: "~~Doped~~ HfO_2 films can exhibit robust ferroelectricity at room temperature, and their compatibility with CMOS processes opens up new possibilities for memories and other ferroelectrics-based devices. Bulk HfO_2 under ambient conditions is monoclinic and paraelectric. Ferroelectricity arises in a metastable orthorhombic phase stabilized in ~~doped~~ HfO_2 nanometric films, typically doped, and prepared under particular conditions."

4: "*[Introduction] "…the orthorhombic phase is formed by rapid thermal annealing*." The polar/Orthorhombic phase is formed even by normal furnace annealing. Adv. Mater. Interfaces 2021, 8, 2100907; https://doi.org/10.1002/admi.202100907, Phys. Status Solidi A2020,217, 1900840; https://doi.org/10.1002/pssa.201900840"

Response: We have removed the word "rapid"

Revised version: In the commonly investigated polycrystalline films, the orthorhombic phase is formed by ~~rapid~~ thermal annealing.

5: "*[introduction] "The possibility of epitaxial growth at lower temperature would be desirable due to its potentially positive impact on the microstructure of the film."*. In this work, the ultra-thin seed layer is grown at 800°C. Does the adverse effect of temperature higher than 700°C not happen in ultra-thin films (2.2 nm seed layer)? If it happens, do the defects or degradation of crystallinity compensate while growing the film (6.6 nm) at 550°C above the seed layer?"

Response: The sentence was not clear and the words "potentially positive impact" could cause confusion. Deposition temperature is a critical parameter affecting the crystallinity, but films grown at lower temperature are expected to have more defects, and our sentence could suggest just the opposite. Thus, we have removed the words "potentially positive" in the sentence. The seed layer, deposited at high temperature, is expected to have a low density of defects, while the top 6.6 nm will have higher amount of defects as lower is the deposition temperature, with impact in the ferroelectric fatigue. We have added a schematic (new Fig. 6) at the end of the Results section.

Revised version: "The possibility of epitaxial growth at lower temperature would be desirable due to its ~~potentially positive~~ impact on the microstructure of the film."

New Fig. 6:

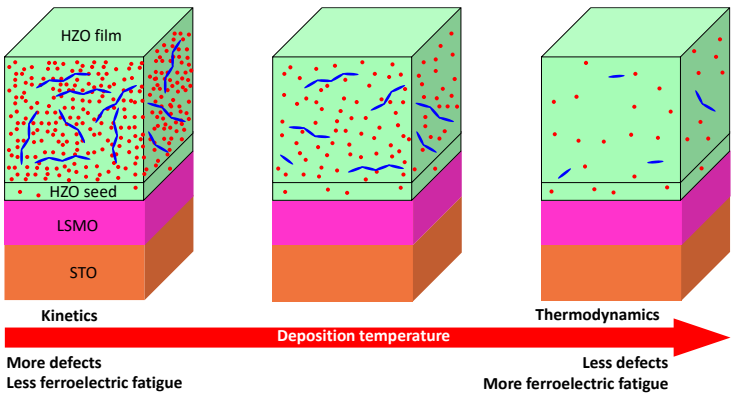

Fig. 6. Schematics of the expected amount of point (red color) and extended (blue color) defects as a function of the deposition temperature.

6: "Do the films grown at 550°C, 600°C, 650°C, 700°C, 750°C and 800°C have exactly same thickness?"

Response: The growth rate of HZO with the PLD conditions used (laser energy and energy density on the PLD target, oxygen pressure, and target-substrate distance) is 0.11 Å/laser pulse. The HZO seed layer and the HZO film are grown in each sample with 200 and 600 laser pulses, respectively, and thus the expected thicknesses are 2.2 and 6.6 nm, and the total HZO thickness 8.8 nm. The real HZO thickness in each sample was determined experimentally by simulation of the o-HZO(111) diffraction peak and the accompanying Laue fringes. The simulation is shown in new Supporting Information S3. Laue fringes are much more evident in the high temperature deposited samples, and thus the thickness of these films is more accurately determined. The total HZO thickness is in the 8.3 - 8.9 nm range (550°C: 8.5 nm, 600°C: 8.7 nm, 650°C: 8.4 nm, 700°C: 8.6 nm, 750°C: 8.3 nm and 800°C: 8.9 nm), in agreement with the expected growth rate.

Revised version: In Experimental: "HZO seed layer was grown at 800 °C and 0.1 mbar of oxygen with 200 laser pulses at a growth rate of 0.11 Å/laser pulse. Next, the seed layer was cooled under 0.1 mbar of oxygen to a temperature T_S in the 550 - 750 °C range, and a HZO film (t ~ 6.6 nm) was grown with 600 laser pulses at...".

In Results, in the paragraph describing Fig. 1: "...at the lowest T_S (600 and 550 °C). The total thickness of the HZO stack (seed layer and film) in each sample was determined by simulation of o-HZO(111) reflection and the Laue fringes (Supporting Information S3). The total HZO thickness in the series of samples ranges from 8.3 to 8.9 nm, in agreement with the expected HZO growth rate of 0.11 Å/laser pulse." The simulation is shown in New Supporting Information S3:

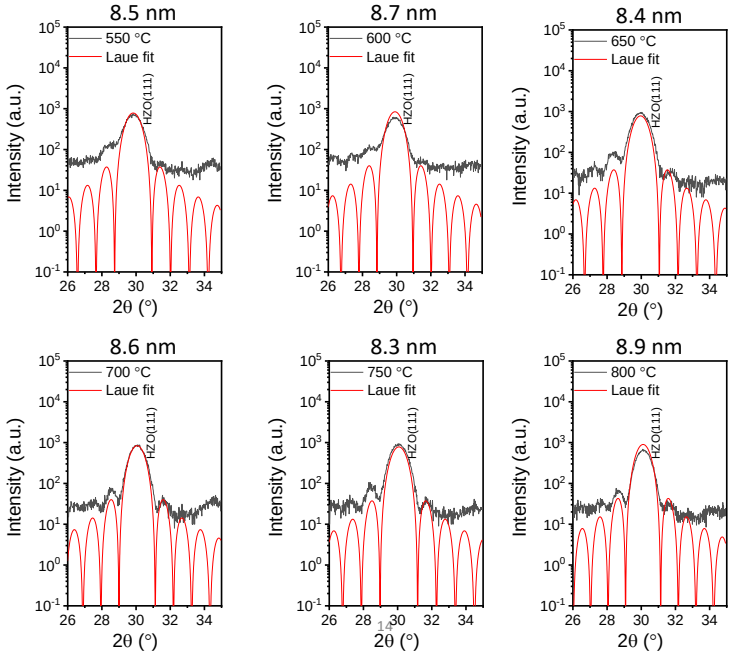

7: "*[introduction] "The possibility of epitaxial growth at lower temperature would be desirable due to its potentially positive impact on the microstructure of the film. Epitaxial films of ferroelectric HfO2 generally present mixture of phases and crystal variants. Microstructure, including polymorphs ratio, crystal grain size and defects, can be critical in the ferroelectric properties of HfO2. However, the high thermal energy required for epitaxy precludes investigating low temperature conditions that could influence the stabilization of the orthorhombic phase and tailor the microstructure of the films."* The microstructure of the films is important and the authors also stated the same as above. It is important to compare the microstructure of the films while comparing the polarization. However, the authors did not present any data and discussion on the microstructure of the films."

Response: The XRD θ-2θ scans presented in the submitted manuscript show degradation of the crystallinity for low-temperature deposition. The XRD scans (Fig.1) show that decreasing Ts the o-HZO(111) peak height decreases and that the Laue oscillations are less evident. The crystalline reduction is quantified in Fig. 2a (XRD intensity) and Fig. 2b (d(111) lattice parameter). The expansion of the HZO crystal lattice, shown in Fig. 2 with the monotonic increase of d(111) as Ts reduces, signals the increased amount of point defects, as reported in ref. T. Song et al., J. Mater. Chem. C, 2022, 10, 1084. Defects are sketched in new Fig. 6. Point defects, as well as other defects located in small volumes or constituting a small fraction of the sample, are hard to be analyzed by techniques as TEM. In the revised version we present XRD measurements (new Supporting Information S2), using a 2D detector, that show presence of minority monoclinic phase, (-111)-oriented, only in the low T_S films.

Revised version: "XRD measurements with a 2D detector are shown in Supporting Information S2. The o-HZO(111) reflection is a bright spot in all the samples, without broadening along the χ angle. There is an additional Bragg spot at around 2θ = 28.5° in the T_S = 550 °C film. The 2θ position and the elongation along χ indicates that corresponds to the monoclinic (m) HZO(-111) reflection [9,13]. The m-HZO(-111) spot decreases with intensity increasing T_S, and it is not detected in the films deposited at T_S higher than 650 °C. In the films deposited at the highest T_S, 750 and 800 °C, the sharp spot at a close position is a Laue fringe of the o-HZO(111) reflection."

8: "The HZO films on STO with seed layer (2.2 nm) have a total thickness of around (2.2+6.6) nm. How thick are the HZO films on STO without a seed layer? Are they ~6.6 nm or ~8.8 nm?"
Response: This important information was not indicated in the submitted manuscript. The films without a seed layer were deposited with 800 laser pulses, and their thickness is ~8.8 nm. We include this information in the revised version.
Revised version: "..., without a seed layer (black squares), and having the same total thickness (~8.8 nm)..."

9: "Information about thickness measurement method and results/data should be added (if not in the main text, can be added in the supplementary)."
Response: This is now done, as indicated in the response to your Comments #6 and #8.

10: "There are three series of samples: (1) HZO on Si (2) HZO (without a seed layer) on STO/LSMO (3) HZO (with HZO seed layer) on STO/LSMO. The HZO seed layer is grown at 800°C. In fig. 2, the only difference between red triangles (with seed layer) and black squares (without seed layer) is the seed layer which is also HZO grown at 800°C. Why do the data of these two at 800°C are different?"

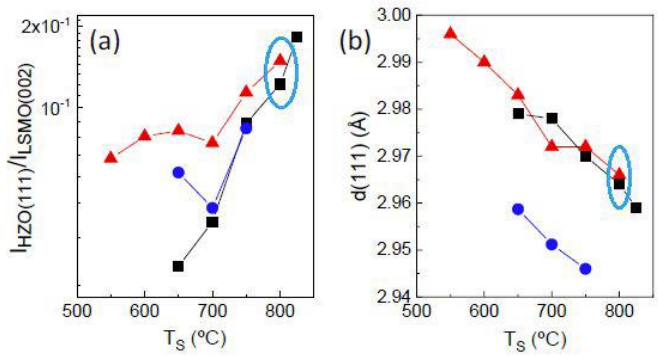

Response: We note that the difference in $I_{HZO(111)}/I_{LSMO(002)}$ values of the two T_S= 800 samples is relatively small (0.149 in the sample with seed layer and 0.122 in the film deposited without a seed layer (reported in reference 11). Moreover, we note that the seed layer was keep under the deposition conditions (800 ºC and 0.1 mbar of O_2) during 18 min, similar to the other seed layers (for which a time was needed to reduce the temperature). Annealing of a 2.2 nm could improve crystal quality of the seed layer, with impact on the 6.6 nm film deposited on top. However, we note that the difference in $I_{HZO(111)}/I_{LSMO(002)}$ values is small, and also small differences in the LSMO thickness can contribute.
Revised version: In the paragraph where Fig. 2b is discussed we have added "The T_S = 800 °C sample with seed layer has slightly higher normalized intensity than the corresponding film without seed layer, which could be caused by the 18 min dwell time."

11: "Similarly, are not HZO (without a seed layer) grown at 800°C and HZO (with HZO seed layer grown at 800°C) grown at 800°C technically the same sample? Should not the polarization data of these two be the same?"

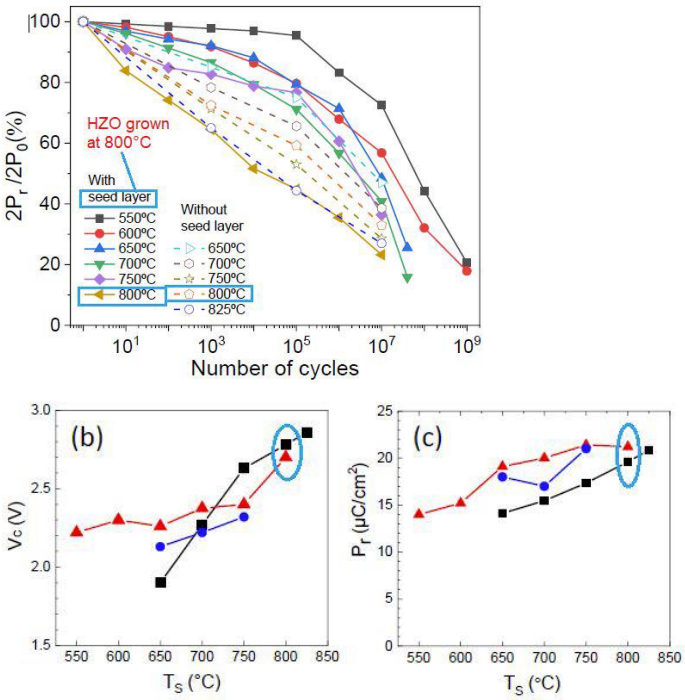

Response: V_C and P_r values (Fig. 3b and c) are similar in the two T_s = 800 samples. In the case of fatigue, the T_S = 800 ºC with seed layer is very similar to the 825ºC sample without seed layer. Moreover, as mentioned in the response to the previous comment, the 18 min dwell time could improve the crystallinity, thus being both T_S = 800 samples not completely equivalent.

12: "The stated facts in the introduction, observations and discussion are not properly correlatable

[introduction] "Annealing at excessively high temperature1,2 or with excessively long time3 promotes the formation of the stable monoclinic phase."

[introduction] "The possibility of epitaxial growth at lower temperature would be desirable due to its potentially positive impact on the microstructure of the film."

Thus, the authors tried to reduce the growth temperature/TS. Decreasing the TS reduces the crystallinity/intensity (o-phase) as seen in fig. 1, 2 and as stated in the discussion (quoted below).

[Results] "The normalized intensity of the films on STO decreases with lowering TS to 700 °C, and shows less dependence for TS between 700 and 550 °C."

However, lowering the TS by using the seed layer leads to enhanced endurance /reduced fatigue. To explain the origin of this positive outcome, the authors considered the coexistence of orthorhombic and monoclinic phases.

[Results/Discussion] "We recently showed that parasitic monoclinic phase has a positive effect on endurance, with less fatigue in films with coexisting orthorhombic and monoclinic phases than in almost pure orthorhombic films25."

Thus, a systematic variation of m-phase with TS must be assumed or observed. But there is no such fact was observed.

[Results] "A tiny peak around 34.5°, is barely observed, corresponding to the position of the HZO{002} reflections of the monoclinic (m) phase. The peak, of very low intensity, is observed only in some films, without correlation with TS."

Response: There were some ambiguities in the previous version that we hope have been clarified as detailed in the response to the previous comments. We have also have rephrased some sentences in the last paragraph of Results to make the text more clear. In our previous publication, T. Song et al., *Adv. Electr. Mater.* 2021, **8**, 2100420, we reported the strong positive effect of the monoclinic phase on the endurance. There we compared films grown on STO (having both phases, like in the films we report here) and scandate substrates (almost free of

monoclinic phase). Here, the differences in the amount of monoclinic phase between films, although detected, is less relevant. We propose, based on the XRD characterization, that the increased amount of defects and increased fraction of monoclinic phase in low T_S samples makes more effective the suppression of pinned domains and thus fatigue is reduced.
Revised version: In addition of the changes detailed in the response to the previous comments, we have rephrased some sentences in the last paragraph of Results: "... using a HZO seed layer, in comparison with films without it, allows enhancing crystalline quality, polarization and...", "... Therefore, point and extended defects in films grown at low temperature (Fig. 6) do not negatively affect endurance and,...", "... with less fatigue in films on STO substrates with coexisting orthorhombic and monoclinic phases than in almost pure orthorhombic films on scandate substrates (Song et al., 2021).", and " Here, in films grown at lower temperature, a greater amount of monoclinic phase, extended defects and more defective grain boundaries between orthorhombic and monoclinic phases could help to suppress the rapid propagation of pinned domains.

13: "The observation of the no wakeup effect is not explained in the discussion."
Response: We have added a short discussion in Results, in the paragraph where the absence of wake-up in indicated. Four new references are cited.
Revised version: There is not wake-up effect in these epitaxial capacitors~~, unlike polycrystalline HfO_2 which usually have it~~. Wake-effect is usually pronounced in polycrystalline films, and it proposed to be caused by oxygen vacancies redistribution or electric-field induced phase transformations [2,27]. Epitaxial films of doped HfO_2 typically are wake-up free, or a very low wake-up effect [9,28,29] which can be due to the lower amount of defects in epitaxial films. The..."
New references:
[2] M.H. Park et al., MRS Commun. 2018, 8, 795.
[27] P. Jiang et al., Adv. Electron. Mater. 2020, 7, 2000728.
[28] J.P. Silva et al., Appl. Mater. Today 2022, 26, 101394.
[29] F. Cüppers et al., Nano Convergence 2022, 9, 26

Reply to Referee 2.
Referee #2: "In this manuscript, the authors show different ways of growing Hf0.5Zr0.5O2 thin films. The XRD, P-E and fatigue properties of the films at different temperatures are also obtained. However, there are some larger points that need to be address before further confirm the outcomes, shown as following points."
Response: Thanks for the detailed and the comments. We have revised the manuscript accordingly.
1: "The authors mention in the title that the HZO film is epitaxially grown, so how to prove that the structure is epitaxially grown film that? The reviewer thinks that the authors should further prove that the film is epitaxial growth method, generally characterization means like Phi sweep and TEM can prove epitaxial film (For example, Adv. Mater. 2022, 34, 2110343 and Adv. Funct. Mater. 2018, 1806037)."
Response: The experimental demonstration of epitaxy is important, particularly considering that some of the films are grown at substrate temperatures much lower than in previous reports. We have measured pole figures around asymmetrical reflections and we confirm that films, even the deposited at the lowest temperature (550 °C), are epitaxial.
Revised version: In the first paragraph of Results, we indicate now "... Epitaxial stabilization of the ferroelectric phase of HZO on LSMO electrodes usually requires deposition temperature above around 700 °C [9–13,18]. Pole figures (Fig. 1c) and ϕ-scans (Fig. 1c) around asymmetrical o-HZO(-111) reflections confirm that the film grows epitaxially, even at T_S = 550 °C is epitaxial (pole figures of the T_S = 650 °C and 800 °C samples are in Supporting Information S1). The films show

the epitaxial relationship and four sets of crystal variants usual in the epitaxial growth on LSMO(001) [9]."

New panels (b) and (c) have been included in the revised Fig. 1:

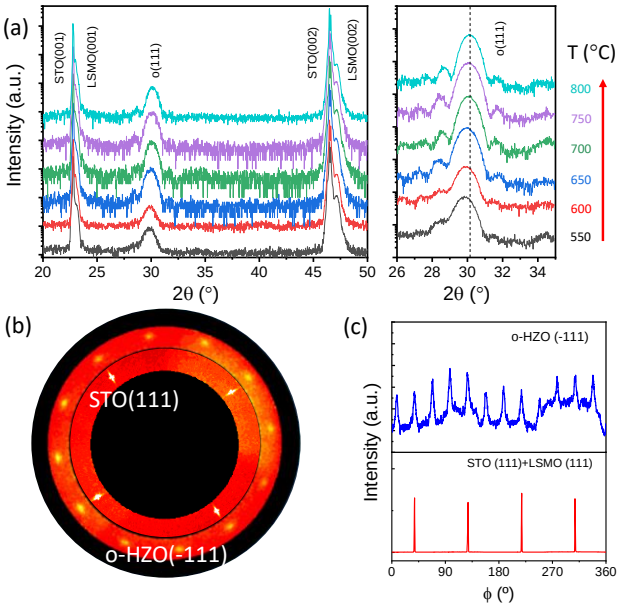

Fig. 1. "... (b) Pole figures and (c) ϕ-scans around o-HZO(-111) and STO(111) reflections of the T_S = 550 °C sample."

New reference is added:

[18] H.Y. Joong, H. Wu, J. Zhao, H. Wang, R. Guo, J. Xiao, B. Zhang, P. Yang, S. J. Pennycook, N. Deng, X. Yan, and J. Chen, Adv. Funct. Mater. 2018, **28**, 1806037.

New Supporting Information S1:

Pole figures (top panels) and ϕ-scans (bottom panels) around asymmetrical o-HZO(-111) and STO(111) reflections of the (a) T_S = 550 °C, (b) T_S = 650 °C, and (c) T_S = 800 °C samples.

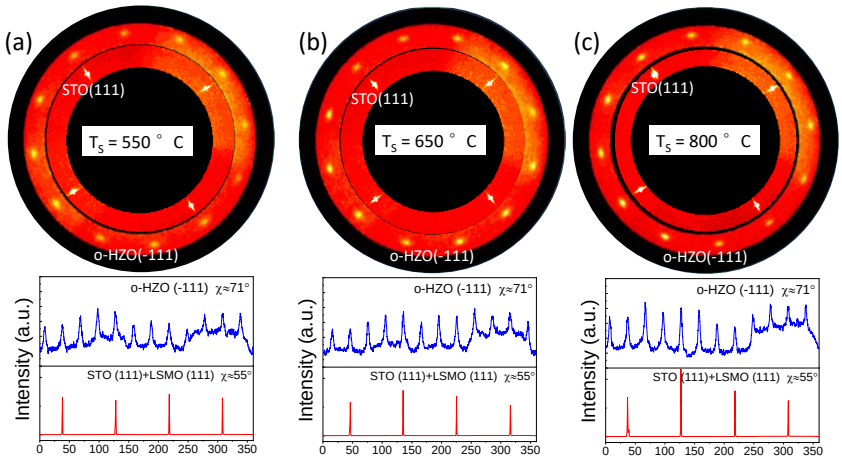

2: "In the experimental section, the authors suggest that the thickness of the grown seed layer is 2.2 nm, and the reviewer thinks that the authors need to prove the thickness of the film and should provide data such as TEM. The reviewer also wondered how the thickness of the grown seed layer affects the crystallinity and ferroelectricity of the film."

Response: The growth rate of HZO per laser pulse depends on laser energy, laser fluence, pressure during deposition, target-substrate distance. All these parameters were fixed in the

growth of the films, and a polished area of the target was scanned in each process. Thus, the thickness of the films is proportional to the number of laser pulses. The HZO seed layer were deposited with 200 pulses, and sequentially, in the same PLD process, the HZO film with 600 additional pulses. This information in detailed in the revised version. The total thickness of HZO (seed layer plus film) was determined by simulation of the o-HZO(111) diffraction peak and Laue fringes, as detailed in the response to Comment #6 or Reviewer #1. The growth rate is 0.11 Å/laser pulses, indicating that the thickness of the seed layer is 2.2 nm. We have not performed TEM of these samples, but we expect little contrast at the interface between the HZO seed layer and the HZO film, which was made very challenging to estimate the seed layer thickness. About the effect of the thickness of the seed layer, we expect a minimum thickness to be an effective seed layer. The threshold thickness, less than 2.2 nm, has not been determined. With a thinner seed layer we do not expect qualitative difference respect the results reported in our manuscript.
Revised version: Please see the response to Comment #6 of Reviewer #1.

3: "The XRD in Figure 1 is mislabeled around 23°, and the reviewer thinks it should be (001) here (such as Sci. China Mater. (2022). doi.org/10.1007/s40843-022-2237-2). Please ask the authors to confirm again."
Response: Thanks for noticing the indexation error. We have corrected it.
Corrected figure in the revised version:

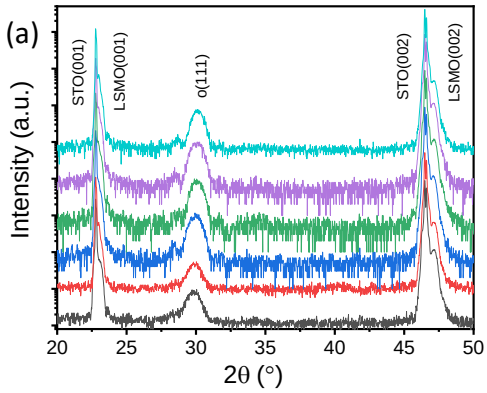

4: "There is a peak between 28° and 29° in the right panel of Figure 1, and it becomes more pronounced with higher temperatures, which the authors should mark and explain."
Response: The peak is a Laue oscillation, very evident in the high T_S films as the reviewer notices. This reflects the better crystallinity of these films. We have rewritten the sentence where this was mentioned.
Revised version: In Results, the sentence "The o-HZO(111) reflection from all the films is accompanied by Laue fringes, indicating good crystalline quality and flat interfaces, less evident in the films grown at the lowest T_S (600 and 550 °C)." is replaced by "The o-HZO(111) reflection from all the films is accompanied by Laue fringes, more pronounced in the films deposited at higher temperature, indicating better crystalline quality and flatter interfaces."

5: "For the data in Figure 2, the reviewers have the following questions: firstly, why did the authors choose the ratio of HZO to LSMO? Secondly, the trend of the data derived from Figure 2 is something that needs to be reconfirmed because LSMO is the grown film and the crystallinity of LSMO film also affects the quality of HZO film formation. So the authors need to give more convincing data characterization when exploring the crystalline strength of HZO films with different growth conditions should be given."
Response: The intensity of the o-HZO(111) peak can depend on the X-ray spot on the sample (affected by the area of the sample that is irradiated and X-ray spot intensity on the sample).

This potential error is greatly reduced by normalizing the o-HZO(111) intensity to the LSMO(002) intensity. The LSMO electrodes used in all the samples reported here were grown using exactly the same deposition parameter, and therefore we expect that all LSMO electrodes have the same crystallinity.
Revised version: In the description of Figure 2, we indicate "...the intensity of the o-HZO(111) peak, normalized to the LSMO(002) peak to compensate potential differences in the XRD measurement conditions of the samples, of films..."

6: "In the description of Figure 3: "In all samples, the imprinted voltage corresponding to the internal electric field pointing to the bottom LSMO electrode is between 0.45 and 0.90 V." How did this conclusion come about? The reviewers would like further explanation from the authors."
Response: The text is not clear in this regard. We have rewritten it.
Revised version: "It can be observed that all the loops are shifted towards the left between 0.45 and 0.90 V. This indicates that in all samples the imprint electric field is towards the LSMO electrode."

7: "The authors showed only the PE plot in the manuscript, but when discussing the remaining polarization values, the reviewer suggested the authors to add a PUND plot."
Response: As the reviewer suggests, we have performed PUND measurements with 1 s delay time. These are plotted in new Supporting Information S7(a). The first observation is that the coercive field in PUND measurements is larger than for dynamic measurements. This coercive field increase is clear from the comparison of the loops collected with dynamic and PUND methods shown in Supporting Information S7(b). This is a result of the presence of the so-called fluid imprint field [P. Buragohain et al., ACS Appl. Mater. Interfaces 2019, 11, 35115–35121, https://doi.org/10.1021/acsami.9b11146]. Therefore, the polarization might not be fully saturated at the maximum applied electric field and remanent polarization might be underestimated. Larger electric field can not be applied because it results in device breakdown. Therefore, the extracted P_r values by PUND are smaller than those obtained from dynamic measurements. It can be inferred by the shapes of the P-E loops dynamic loops that the extrinsic contributions are residual. In any case the trends are the same and the conclusions of the manuscript are not altered [Supporting Information S7(c)]
Revised version: We have included the new PUND measurements in new Supporting Information S7 with their description. We have included the following sentence in the main text: Similar trend is observed if P_r values are obtained from PUND measurements Supporting Information S7). "
New Supporting Information S7:
In Figure S7(a), the PUND loops measured with 1 s delay time for all the studied samples are shown. Similar Pr values are obtained. In Figure S7(b), a comparison of the loops obtained with dynamic and PUND methods for a representative sample (T_s = 750 ^oC) is shown. It can be observed that the coercive field is larger for the PUND loop. This results from the presence of the fluid imprint field [1]. The increase of coercive field does not allow to fully saturate the polarization of the sample at the used maximum applied electric field. Larger electric field results on device breakdown. In Figure S7(c), it can be observed that the P_r obtained using PUND is slightly less than those obtained by dynamic method. In both cases the trend is the same indicating that the decrease of polarization while decreasing T_S is small.

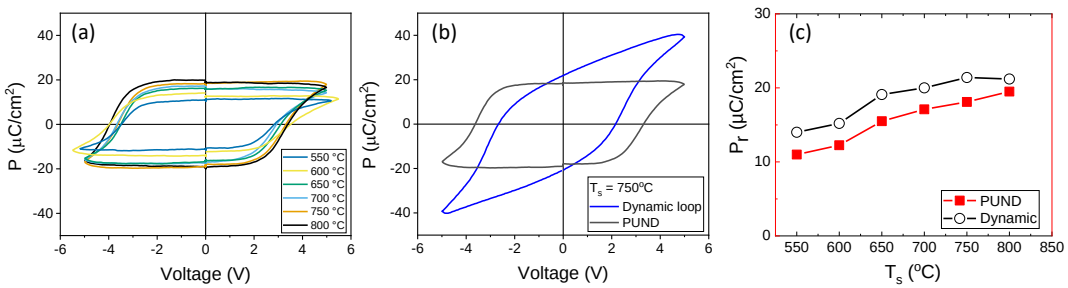

8: "The authors grow HZO films in two steps, the first step is growing the seed layer. The reviewer thinks that the authors should explain in detail the purpose of growing the seed layer and its principle should be analyzed."

Response: When HZO grows on LSMO, the interface energy is high and epitaxy requires high TS. However, if HZO grows on an epitaxial seed HZO, there is not interface energy between the HZO film deposited in the second step and the HZO seed layer deposited in the first step. This process of homoepitaxy requires less energy and can occur at lower T_S.

Revised version: We have extended the explanation in the last paragraph of Introduction: "...Films were grown in two steps. In the first step, an ultra-thin seed layer is grown at optimal high temperature (800 °C) for heteroepitaxial growth of HZO [9–13]. The HZO growth then continues (second step) at a lower temperature on the epitaxial HZO seed layer. Homoepitaxial growth is expected to be possible at lower temperature, since there is not a HZO film / HZO seed layer interface energy contribution, in contrast with the high interface energy at the HZO seed layer / substrate interface. We will show that... "

9: ""Doped HfO2 films exhibit robust ferroelectricity at room temperature, and their compatibility with CMOS processes opens up new possibilities for memories and other ferroelectrics-based devices." The reference should be cited there (such as Adv. Funct. Mater. 2021, 31, 2006773.)."

Response: The reference and a second one is cited in the revised version

Revised version: "...for memories and other ferroelectrics-based devices [1,2].

New references are added:

[1] K. Sun et al., Adv. Funct. Mater. 2021, 31, 2006773.

[2] M.H. Park et al., MRS Commun. 2018, 8, 795.

Reply to Editorial comments.

1: "A table of contents entry: graphic maximum size 8 cm x 4 cm and 1-2 sentence(s) of editable text, with a maximum of 250 characters (including spaces), highlighting the key findings of the work. It is recommended authors make use of the full space available for the graphic."

Response: The Table (244 characters) and the graphic is provided.

Graphic:

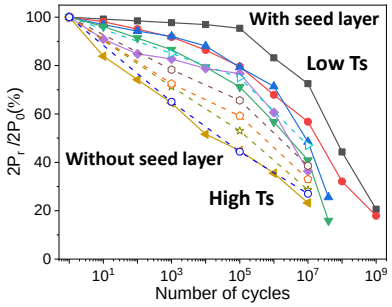

Table of contents: A seed layer of thickness about 2 nm allows reducing in the threshold temperature for epitaxy of $Hf_{0.5}Zr_{0.5}O_2$ films in at least 200 °C. Films deposited at low temperature on seed layers show reduced ferroelectric fatigue and improved endurance.

ARTICLE

Ferroelectric $Hf_{0.5}Zr_{0.5}O_2$ films with improved endurance by low temperature epitaxial growth on seed layers †

Received 00th January 20xx,
Accepted 00th January 20xx

DOI: 10.1039/x0xx00000x

Tingfeng Song,[a] Romain Bachelet,[b] Guillaume Saint-Girons,[b] Ignasi Fina,*[a] and Florencio Sánchez*[a]

The crystallization temperature is a critical parameter in the stabilization of the metastable ferroelectric phase of HfO_2. The optimal crystallization temperature used for polycrystalline films is too low to grow epitaxial films. We have developed a new growth strategy, based on the use of an ultrathin seed layer, to obtain high-quality epitaxial films of orthorhombic $Hf_{0.5}Zr_{0.5}O_2$ at lower temperature. The threshold temperature for epitaxy is reduced from about 750 °C to about 550 °C by using a seed layer. Epitaxial films deposited at low temperature exhibit highly enhanced endurance, and films grown at 550 - 600 °C have high polarization, no wake-up effect, and greatly reduced fatigue and improved endurance in comparison with the films deposited at high temperature without a seed layer. We propose that the endurance enhancement is due to a positive effect of the defects, which limit the propagation of pinned ferroelectric domains.

1. Introduction

HfO_2 films can exhibit robust ferroelectricity at room temperature, and their compatibility with CMOS processes opens up new possibilities for memories and other ferroelectrics-based devices[1,2]. Bulk HfO_2 under ambient conditions is monoclinic and paraelectric. Ferroelectricity arises in a metastable orthorhombic phase stabilized in HfO_2 nanometric films, typically doped, and prepared under particular conditions. In the commonly investigated polycrystalline films, the orthorhombic phase is formed by thermal annealing. Annealing at excessively high temperature [3,4] or with excessively long time [5] promotes the formation of the stable monoclinic phase. It is proposed that the stabilization of the metastable ferroelectric phase is due to a combined effect of the surface energy contribution and kinetic limitations [6]. Before annealing, the quasi-amorphous films would have small orthorhombic nuclei. During annealing, the nanocrystals transform to tetragonal phase that is stable at high temperature. However, when the crystal grains increase in size, the lowest energy corresponds to the monoclinic phase. However, the energy barrier for this phase transformation is high, and the transformation is kinetically suppressed in $Hf_{0.5}Zr_{0.5}O_2$ (HZO) films if annealing is short and at moderate temperature. It has also been reported that monoclinic phase can be transformed to tetragonal and orthorhombic phases by very high temperature annealing (1000 - 1200 °C) in solid phase epitaxy of Y-doped HfO_2 films [7]. Therefore, in crystallization of quasi-amorphous films, annealing temperature is a critical parameter to stabilize the metastable orthorhombic phase rather than the thermodynamically stable monoclinic phase.

Epitaxial growth from a vapor phase radically differs from crystallization processes by annealing. Diffusion of atoms on a surface and chemical bonding at specific positions generally requires high thermal energy, suitable saturation conditions, and a growth rate low enough to limit crystalline defects. In particular, the ferroelectric phase of doped HfO_2 has been stabilized in epitaxial films, mainly by pulsed laser deposition, and with substrate temperature around 700-800 °C [8–12]. The study of the window for epitaxial growth of ferroelectric HZO films revealed a severe reduction in crystallinity for temperature (substrate heater block) below around 700 °C [13]. The possibility of epitaxial growth at lower temperature would be desirable due to its impact on the microstructure of the film. Epitaxial films of ferroelectric HfO_2 generally present mixture of phases and crystal variants. Microstructure, including polymorphs ratio, crystal grain size and defects, can be critical in the ferroelectric properties of HfO_2. However, the high thermal energy required for epitaxy precludes investigating low-temperature conditions that could influence the stabilization of the orthorhombic phase and tailor the microstructure of the films.

In the heteroepitaxial growth, the interface energy is an important factor in the formation of crystal nuclei and in determining the crystal polymorphs that nucleate. We have investigated a new strategy to grow ferroelectric HfO_2 films, with the aim of widening the window for epitaxial growth at

[a] Institut de Ciència de Materials de Barcelona (ICMAB-CSIC), Campus UAB, Bellaterra 08193, Barcelona, Spain. E-mail: ifina@icmab.es, fsanchez@icmab.es
[b] Univ. Lyon, Ecole Centrale de Lyon, INSA Lyon, Université Claude Bernard Lyon 1, CPE Lyon, CNRS, Institut des Nanotechnologies de Lyon - INL, UMR5270, 69134 Ecully, France.

†Electronic Supplementary Information (ESI) available: XRD Pole figures. XRD 2θ - χ maps measured with 2D detector. Simulation of Laue fringes. XRD θ-2θ scans of HZO films deposited on Si(001). Current-voltage loops measured in the HZO films deposited on STO(001). Current - voltage and corresponding polarization - voltage loops of the HZO films deposited on Si(001). PUND measurements. Polarization – voltage loops measured in the pristine state and after the indicated number of cycles. Polarization retention measurements for films on STO(001). Leakage current curves measured in the pristine state and after the indicated number of cycles. See DOI: 10.1039/x0xx00000x

lower temperature. Films were grown in two steps. In the first step, an ultra-thin seed layer is grown at optimal high temperature (800 °C) for heteroepitaxial growth of HZO [9–13]. The HZO growth then continues (second step) at a lower temperature on the epitaxial HZO seed layer. Homoepitaxial growth is expected to be possible at lower temperature, since there is not a HZO film / HZO seed layer interface energy contribution, in contrast with the high interface energy at the HZO seed layer / substrate interface. We will show that the use of the seed layer allows the stabilization of the orthorhombic phase at a lower temperature. The films grown at low temperature (550 - 600 °C) show excellent ferroelectric properties: slightly reduced ferroelectric polarization, absence of wake-up effect and greatly enhanced robustness against fatigue.

2. Experimental

Top ferroelectric HZO films and bottom $La_{0.67}Sr_{0.33}MnO_3$ (LSMO) electrodes were grown on (001)-oriented $SrTiO_3$ (STO) substrates in a single process by pulsed laser deposition (PLD) using a KrF excimer laser (248 nm wavelength). The LSMO electrodes, thickness t ~ 25 nm, were grown at T_S = 700 °C and oxygen pressure P_{O2} = 0.1 mbar. HZO films were then grown in two steps. First, an ultra-thin (t ~ 2.2 nm) HZO seed layer was grown at 800 °C and 0.1 mbar of oxygen with 200 laser pulses at a growth rate of 0.11 Å/laser pulse. Next, the seed layer was cooled under 0.1 mbar of oxygen to a temperature T_S in the 550 - 750 °C range, and a HZO film (t ~ 6.6 nm) was grown with 600 laser pulses at that temperature and same oxygen pressure and growth rate that the seed layer. Another film was grown at 800 °C, in a two steps process with a dwell time of 18 min after deposition of the first 2.2 nm. At the end of the deposition, samples were cooled under 0.2 mbar of oxygen partial pressure. Another series of films was deposited at 650, 700 and 750 °C on Si(001) buffered with an epitaxial STO layer. Details on STO growth conditions and structural properties are reported elsewhere [14,15].

Structural characterization of the HZO films was performed by X-ray diffraction (XRD) using Cu Kα radiation. Platinum top electrodes, 20 nm thick and 20 µm in diameter, were grown by dc magnetron sputtering through stencil masks for electrical characterization. Ferroelectric polarization loops were measured at 1 kHz using the dynamic leakage current compensation (DLCC) procedure at room temperature in top-bottom configuration [16,17]. Endurance was measured cycling the sample at 100 kHz using bipolar square pulses of amplitude of 4.5 V and measuring polarization loops at 1 kHz.

3. Results

Fig. 1a shows XRD θ-2θ scans of the HZO films on STO substrates. The growth temperature (second step) is indicated on the right. The high intensity peaks at 2θ around 23 and 47° correspond to the (001) and (002) reflections from the STO

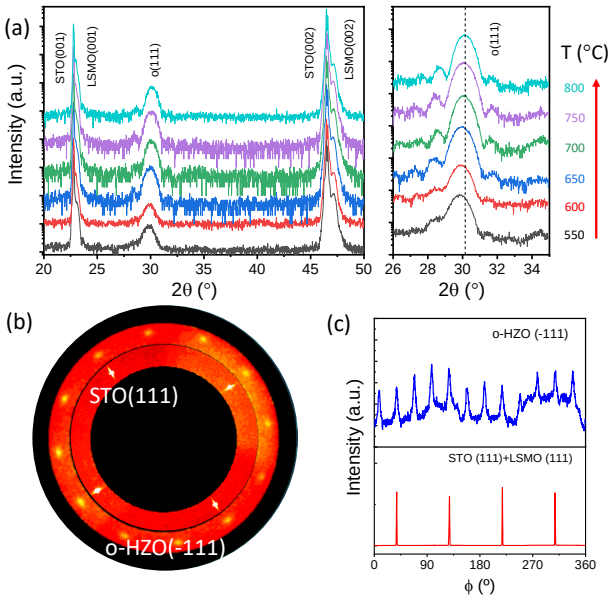

Fig. 1 (a) XRD θ-2θ scans of HZO films deposited on STO(001) at the temperature indicated on the right. Scans are shifted vertically for clarity. The enlarged 2θ region shown in the right panel was scanned with a longer acquisition time. The dashed vertical line marks the position of the peak in the T_S = 800 °C sample. (b) Pole figures and (c) ϕ-scans around o-HZO(-111) and STO(111) reflections of the T_S = 550 °C sample.

substrate. The corresponding reflections from the LSMO electrode lie to the right of the substrate peaks. Furthermore, all samples exhibit a peak at 2θ around 30°, the position of the (111) reflection of the orthorhombic (o) phase of HZO. Therefore, HZO crystallizes over the entire investigated T_S range. The peak is broad, as expected considering that the HZO total thickness is less than 9 nm. Epitaxial stabilization of the ferroelectric phase of HZO on LSMO electrodes usually requires deposition temperature above around 700 °C [9–13,18]. Pole figures (Fig. 1c) and ϕ-scans (Fig. 1c) around asymmetrical o-HZO(-111) reflections confirm that the film grows epitaxially, even at T_S = 550 °C is epitaxial (pole figures of the T_S = 650 °C and 800 °C samples are in Supporting Information S1). The films show the epitaxial relationship and four sets of crystal variants usual in the epitaxial growth on LSMO(001) [9]. The right panel in Fig. 1a shows a 2θ zoomed region around the o-HZO(111) reflection, measured with a longer acquisition time. The o-HZO(111) reflection from all the films is accompanied by Laue fringes, more pronounced in the films deposited at higher temperature, indicating better crystalline quality and flatter interfaces. XRD measurements with a 2D detector are shown in Supporting Information S2. The o-HZO(111) reflection is a bright spot in all the samples, without broadening along the χ angle. There is an additional Bragg spot at around 2θ = 28.5° in the T_S = 550 °C film. The 2θ position and the elongation along χ indicates that corresponds to the monoclinic (m) HZO(-111) reflection [9,13]. The m-HZO(-111) spot decreases in intensity with T_S increasing, and it is not detected in the films deposited at T_S higher than 650 °C. In the films deposited at the highest T_S, 750 and 800 °C, the sharp spot at a close position is a Laue fringe of the o-HZO(111) reflection. The total thickness of the HZO stack (seed layer and film) in each sample was determined by

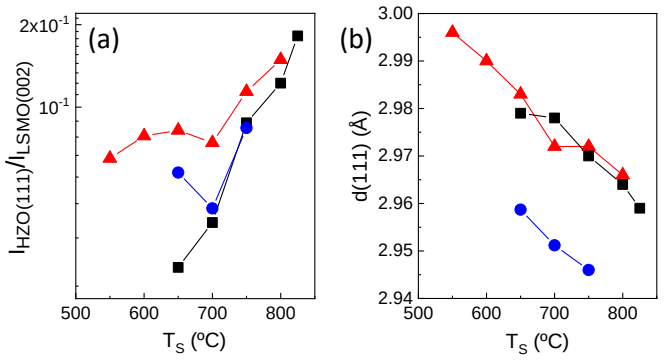

Fig. 2 Intensity of the o-(111) reflection, normalized to that of the LSMO(002) peak (a), and out-of-plane lattice distance corresponding to the o-(111) reflection (b), as a function of deposition temperature T_S for films on STO(001) (red triangles) and Si(001) (blue circles). Black squares are data corresponding to films on STO(001) deposited without a seed layer [13].

simulation of o-HZO(111) reflection and the Laue fringes (Supporting Information S3). The total HZO thickness in the series of samples ranges from 8.3 to 8.9 nm, in agreement with the expected HZO growth rate of 0.11 Å/laser pulse. In Fig. 1, a tiny peak around 34.5°, is also barely observed, corresponding to the position of the HZO{002} reflections of the monoclinic (m) phase. The peak, of very low intensity, is observed only in some films, without correlation with T_S. In contrast, the position of the o-HZO(111) peak varies monotonically with the deposition temperature. The dashed vertical line marks the position of the peak for the T_S = 800 °C sample. It can be seen that as T_S decreases, the peak shifts to a lower angle, indicating that the HZO(111) out-of-plane lattice distance, d(111), increases. To demonstrate that a seed layer is also effective for low-temperature epitaxy on Si(001) substrates, we used epitaxial STO buffer layers, which allow epitaxial growth of LSMO electrodes and HZO ferroelectric films [14]. XRD θ-2θ scans of three films grown at 550, 600 and 650 °C (Supporting Information S4) confirm stabilization of the orthorhombic phase at low T_S, with a similar d(111) - T_S dependence than the films on STO(001).

The intensity of the o-HZO(111) diffraction peak can be used as an approximation to estimate the orthorhombic phase content in the films. Fig. 2(a) shows the intensity of the o-HZO(111) peak, normalized to the LSMO(002) peak to compensate potential differences in the XRD measurement conditions of the samples, of films grown on seed layers on STO (red triangles) and Si (blue circles) substrates. The normalized intensity of the films on STO decreases with lowering T_S to 700 °C, and shows less dependence for T_S between 700 and 550 °C. The intensity-T_S dependence is similar in the three samples on Si, although the normalized intensity is lower. The graph also includes the corresponding normalized intensity of films deposited at various T_S directly on LSMO/STO(001) electrode, without a seed layer (black squares), and having the same total thickness (~8.8 nm) [13]. The T_S = 800 °C sample with seed layer has slightly higher normalized intensity than the corresponding film without seed layer, which could be caused by the 18 min dwell time. The intensity of the films grown without seed layer decreases very sharply with T_S, and is very low for T_S below 750 °C. Fig.2(a) indicates that i) the growth of highly crystalline films below 750 °C is only achieved on seed layers and, ii) for higher temperatures, the use of a seed layer enhances HZO crystallization.

The variation of the position of the o-HZO(111) peak with T_S (Figure 1) is quantified in Fig. 2(b). The lattice parameter d(111) increases monotonically with decreasing T_S (red triangles) to about 1.3%, and matches that of films grown at the same temperature without a seed layer (black squares). The unit cell expansion of a film grown by PLD can be caused by defects that form when the energy of the PLD plasma is high [19–21]. The energy of the atomic species in the PLD plasma reaching the substrate depends on the laser fluence, the target - substrate distance and the gas pressure [22–24]. These parameters were kept constant in the preparation of the films discussed here. However, the number of defects that form in a film depends on the balance between growth kinetics and thermodynamics [25]. This balance, as demonstrated recently in the epitaxial growth of $BaTiO_3$ films, can be tailored by the substrate temperature [26]. The damage caused by the energetic PLD plasma is reduced by the high thermal energy in HZO films grown at high T_S, while lowering T_S thermal energy is less, leading to more defects and d(111) expansion. The films on Si show the same dependence of d(111) on T_S, but with a reduced value compared to the equivalent films on STO, which is a consequence of the tensile stress caused by the mismatch between thermal expansion

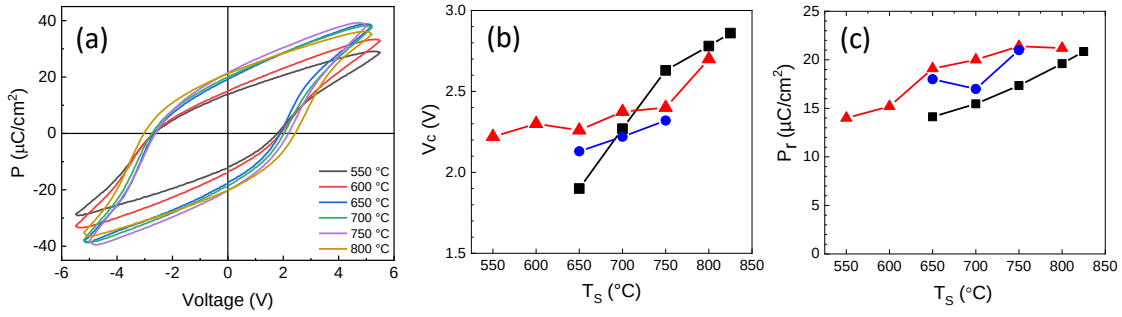

Fig. 3 (a) Ferroelectric polarization loops of HZO films deposited at the temperature indicated at the bottom right. Coercive voltage (b) and remanent polarization (c), as a function of deposition temperature T_S for films on STO(001) (red triangles) and Si(001) (blue circles). Black squares are data corresponding to films on STO(001) deposited without a seed layer [11].

coefficients (TEC) of HZO and Si. Although TEC mismatch effects are less relevant if T_S is lower, the two lineal dependences are parallel, probably because the seed layer is grown in all samples at T_S = 800 °C.

All films are ferroelectric, confirming the stabilization of the orthorhombic phase throughout the T_S range. The polarization loops of the films on STO(001) (Fig. 3(a), with the corresponding current-voltage loops in Supporting Information S5) are shifted towards negative voltage values. The positive coercive voltage V_{C+} increases with T_S from around 1.8 V to 2.4 V, while the negative coercive voltage V_{C-} ranges from -2.7 V to -3.0 V. It can be observed that all the loops are shifted towards the left between 0.45 and 0.90 V. This indicates that in all samples the imprint electric field is towards the LSMO electrode. The average coercive voltage $V_C = (V_{C+} + |V_{C-}|)/2$ is in the range of 2.2 - 2.7 V, increasing with T_S (Figure 3b, red triangles), corresponding to coercive electric field E_C in the 2.5 - 3.1 MV/cm range. The coercive voltage of the three films grown on Si substrate is slightly lower and shows a similar T_S dependence (blue circles). Epitaxial films grown directly on LSMO/STO(001) without a seed layer exhibit similar V_C values and T_S dependence (black squares). High E_C of about 2.5 - 3 MV/cm, which exceeds the usual E_C of polycrystalline films, is common in HZO epitaxial films of similar thickness [11,13]. The remanent polarization is plotted against T_S in Fig. 3(c) (red triangles). P_r decreases moderately with decreasing growth temperature, from 21.2 μC/cm² in the T_S = 800 °C film to 14 μC/cm² in the T_S = 550 °C film. Similar trend is observed if P_r values are obtained from PUND measurements Supporting Information S7). The remanent polarization of the films on Si (polarization loops shown in Supporting Information S6) is comparable (blue circles). In the films deposited without seed layer, the

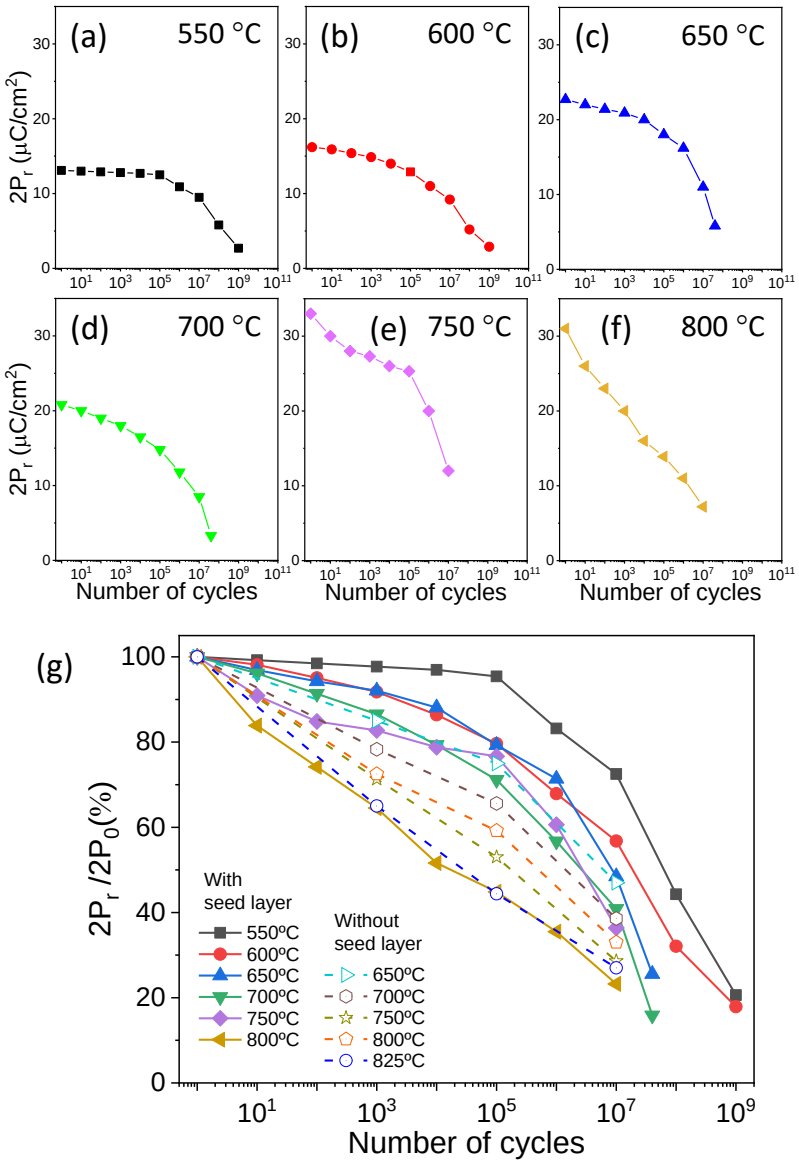

Fig. 4 Endurance, measured with bipolar rectangular pulses of frequency 100 kHz and amplitude 4.5 V, of T_S = 550 °C (a), 600 °C (b), 650 °C (c), 700 °C (d), 750 °C (e), and 800 °C (f) films on STO. (g) Comparison of endurance (remanent polarization is normalized to the pristine state value) of the films grown at various T_S on a seed layer (solid symbols and solid lines) films grown at various T_S without a seed layer (empty symbols and dashed lines). Data of films grown without a seed layer are reported in [24].

polarization is similar in the film deposited at 800 °C, 19.6 μC/cm², but decreases sharply with T_S to around 14 μC/cm² in the T_S = 650 °C film.

Fatigue was investigated by cycling the capacitors with bipolar rectangular pulses of frequency 100 kHz and amplitude 4.5 V, close to the voltage used to obtain saturated loops (Fig. 3(a)). Endurance measurements are shown in Fig. 4(a-f) (see Supporting Information S8 for polarization loops). There is no wake-up effect in these epitaxial capacitors. Wake-up effect is usually pronounced in polycrystalline films, and it proposed to be caused by oxygen vacancies redistribution or electric-field induced phase transformations [2,27]. Epitaxial films of doped HfO_2 typically are wake-up free, or a very low wake-up effect [9,28,29] which can be due to the lower amount of defects in epitaxial films. The T_S = 550 °C film (Fig. 4(a)) has a moderately low $2P_r$ of 13.1 μC/cm² in the pristine state, and there is no significant fatigue over 10^5 cycles ($2P_r$ = 12.5 μC/cm²). $2P_r$ drops to 9.5 μC/cm² after 10^7 cycles, and after 10^9 it is only 2.7 μC/cm². More cycles caused electric breakdown. HZO films grown at higher temperature show fatigue from the beginning, the greater the higher T_S. In the T_S = 600 °C sample (Fig. 4(b)) the decrease in $2P_r$ after 10^5 cycles is low, decreasing from 16.2 to 12.9 μC/cm². Thereafter, fatigue is more pronounced and $2P_r$ is 2.9 μC/cm² after 10^9 cycles, before breakdown occurs. In the T_S = 650 and 700 °C samples (Fig. 4(c, d), respectively), $2P_r$ in the pristine state is greater than 20 μC/cm², but high fatigue begins after fewer cycles and, moreover, breakdown occurs earlier, after 4x10^7 cycles. In the samples grown at the highest temperatures, 750 and 800 °C (Fig. 4(e, f), respectively), with high initial $2P_r$ of more than 30 μC/cm², the degradation of polarization is more evident, and the tendency of early breakdown with increased T_S is confirmed, occurring after 10^7 cycles in both films. Therefore, the films deposited at low temperature, although they have lower polarization in the pristine state, are less affected by fatigue and more robust against breakdown. The polarization is normalized in Fig. 4(g) to compare the endurance of the films grown at various T_S on a seed layer (solid symbols and solid lines). The robustness against fatigue and electrical breakdown at low T_S is evident. The graph also includes data from films grown at various T_S without a seed layer (empty symbols and dashed lines) [30]. The films deposited at low T_S without seed layer already showed less fatigue. However, the crystallization and ferroelectric polarization of films deposited at less than 700 °C was too low. The use of a seed layer, which enhances crystallization, allows for epitaxial growth and high polarization at lower temperature, with a positive impact on fatigue and resistance against breakdown as shown in Fig. 4(g). Moreover, all films in the series show excellent retention, with extrapolated remanent polarization after 10 years above 47% of the initial value for either positive or negative poling (Supporting Information S9).

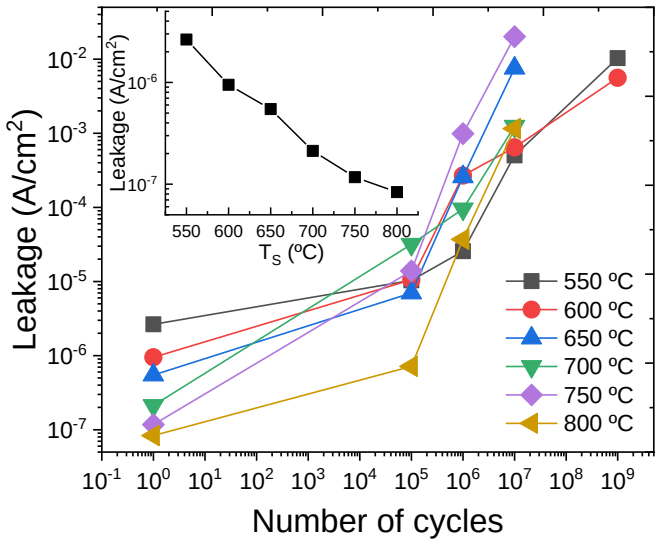

Fig. 5 Evolution of current leakage density with the number of cycles of the films on STO(001) deposited at the temperature indicated at the bottom right. Inset: Pristine state leakage current density of films on STO(001) as a function of deposition temperature.

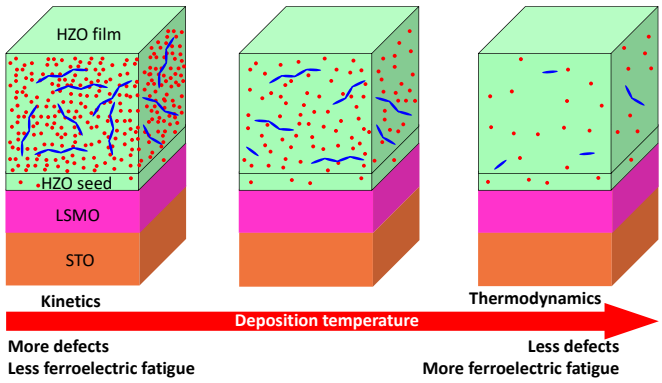

Fig. 6 Schematics of the expected amount of point (red color) and extended (blue color) defects as a function of the deposition temperature.

It has been shown here that using a HZO seed layer, in comparison with films without it, allows enhancing crystalline quality, polarization and resistance against fatigue of ferroelectric HZO films. Also, it has been shown that lowering the growth temperature results in less polarization but also less fatigue. The decrease in polarization is a consequence of the reduced crystallization and the lower amount of orthorhombic phase in films deposited at low T_S. Furthermore, there is a greater expansion of the out-of-plane lattice parameter with decreasing T_S, indicating a higher density of point defects. Domain pinning at point defects is a possible mechanism of fatigue, but the lower fatigue in low T_S films suggests that this is not a primary fatigue mechanism in epitaxial films. On the other hand, low T_S films are less crystalline and may have extended defects. The higher number of point and extended defects in low-temperature deposited films probably causes the monotonic increase of leakage current in pristine state with decreasing deposition temperature (Fig. 5, inset). Leakage (see Supporting Information S10 for leakage curves) increases with cycling in all samples, particularly after 10^5 - 10^6 cycles, but the increase in low T_S films is less and, after 10^7 cycles, the T_S = 550 and 600 °C films have the lowest leakage. This may contribute to the high robustness of low T_S films against electrical breakdown. Therefore, point and extended defects in films grown at low temperature (Fig. 6) do not negatively affect

endurance and, on the contrary, may be a major factor for lower fatigue. We recently showed that parasitic monoclinic phase has a positive effect on endurance, with less fatigue in films on STO substrates with coexisting orthorhombic and monoclinic phases than in almost pure orthorhombic films on scandate substrates [31]. We argued that this is a consequence of the suppression of propagation of pinned domains at the boundaries with the non-ferroelectric phase. Here, in films grown at lower temperature, a greater amount of monoclinic phase, extended defects and more defective grain boundaries between orthorhombic and monoclinic phases could help to suppress the rapid propagation of pinned domains.

4. Conclusions

In conclusion, the use of a seed layer allows the epitaxial growth of enhanced ferroelectric HZO films on STO(001) and Si(001) at significantly lower temperature. The orthorhombic phase forms over a wide temperature range, with the (111) out-of-plane lattice parameter decreasing linearly with deposition temperature by about 1.3%. The crystallization of the orthorhombic phase is reduced with decreasing substrate temperature and the polarization is slightly reduced. However, the films grown at low temperature are more robust against ferroelectric fatigue and electrical breakdown. The results suggest that the pinning of ferroelectric domains at point defects is not a major mechanism of fatigue. The suppression of pinned domain propagation at more defective regions and grain boundaries in low-temperature deposited films is proposed as the reason of the enhancement.

Conflicts of interest

There are no conflicts to declare.

Acknowledgements

Financial support from the Spanish Ministry of Science and Innovation (MCIN/AEI/ 10.13039/501100011033), through the Severo Ochoa FUNFUTURE (CEX2019-000917-S), PID2020-112548RB-I00 and PID2019-107727RB-I00 projects, and from CSIC through the i-LINK (LINKA20338) program is acknowledged. We also acknowledge project TED2021-130453B-C21, funded by MCIN/AEI/10.13039/501100011033 and European Union NextGeneration EU/PRTR. TS is financially supported by China Scholarship Council (CSC) with No. 201807000104. TS work has been done as a part of his Ph.D. program in Materials Science at Universitat Autònoma de Barcelona. RB and GSG acknowledge financial support from the French national research agency (ANR) through the projects DIAMWAFEL (No. ANR-15-CE08-0034), LILIT (No. ANR-16-CE24-0022), and MITO (No. ANR-17-CE05-0018), as well as P. Regreny, C. Botella, and J. B. Goure for the technical support.

References

1 K. Sun, J. Chen and X. Yan, *Adv Funct Mater*, 2021, **31**, 2006773.

2 M. H. Park, Y. H. Lee, T. Mikolajick, U. Schroeder and C. S. Hwang, *MRS Commun*, 2018, **8**, 795–808.

3 M. Hyuk Park, H. Joon Kim, Y. Jin Kim, W. Lee, T. Moon and C. Seong Hwang, *Appl Phys Lett*, 2013, **102**, 242905.

4 H. A. Hsain, Y. Lee, G. Parsons and J. L. Jones, *Appl Phys Lett*, 2020, **116**, 192901.

5 J. Wang, D. Zhou, W. Dong, Y. Yao, N. Sun, F. Ali, X. Hou and F. Liu, *Adv Electron Mater*, 2021, **7**, 2000585.

6 M. H. Park, Y. H. Lee, T. Mikolajick, U. Schroeder and C. S. Hwang, *Adv Electron Mater*, 2019, **5**, 1800522.

7 Y. Tashiro, T. Shimizu, T. Mimura and H. Funakubo, *ACS Appl Electron Mater*, 2021, **3**, 3123–3130.

8 T. Shimizu, K. Katayama, T. Kiguchi, A. Akama, T. J. Konno, O. Sakata and H. Funakubo, *Sci Rep*, 2016, **6**, 32931.

9 J. Lyu, I. Fina, R. Solanas, J. Fontcuberta and F. Sánchez, *Appl Phys Lett*, 2018, **113**, 082902.

10 P. Nukala, Y. Wei, V. de Haas, Q. Guo, J. Antoja-Lleonart and B. Noheda, *Ferroelectrics*, 2020, **569**, 148–163.

11 I. Fina and F. Sánchez, *ACS Appl Electron Mater*, 2021, **3**, 1530–1549.

12 Y. Wang, Q. Wang, J. Zhao, T. Niermann, Y. Liu, L. Dai, K. Zheng, Y. Sun, Y. Zhang, J. Schwarzkopf, T. Schroeder, Z. Jiang, W. Ren and G. Niu, *Appl Mater Today*, 2022, **29**, 101587.

13 J. Lyu, I. Fina, R. Solanas, J. Fontcuberta and F. Sánchez, *ACS Appl Electron Mater*, 2019, **1**, 220–228.

14 J. Lyu, I. Fina, R. Bachelet, G. Saint-Girons, S. Estandía, J. Gázquez, J. Fontcuberta and F. Sánchez, *Appl Phys Lett*, 2019, **114**, 222901.

15 G. Saint-Girons, R. Bachelet, R. Moalla, B. Meunier, L. Louahadj, B. Canut, A. Carretero-Genevrier, J. Gazquez, P. Regreny, C. Botella, J. Penuelas, M. G. Silly, F. Sirotti and G. Grenet, *Chemistry of Materials*, 2016, **28**, 5347–5355.

16 I. Fina, L. Fàbrega, E. Langenberg, X. Martí, F. Sánchez, M. Varela and J. Fontcuberta, *J Appl Phys*, 2011, **109**, 074105.

17 R. Meyer, R. Waser, K. Prume, T. Schmitz and S. Tiedke, *Appl Phys Lett*, 2005, **86**, 142907.

18 H. Y. Yoong, H. Wu, J. Zhao, H. Wang, R. Guo, J. Xiao, B. Zhang, P. Yang, S. J. Pennycook, N. Deng, X. Yan and J. Chen, *Adv Funct Mater*, 2018, **28**, 1–10.

19 T. Song, R. Solanas, M. Qian, I. Fina and F. Sánchez, *J Mater Chem C Mater*, 2022, **10**, 1084–1089.

20 R. Takahashi, T. Yamamoto and M. Lippmaa, *Cryst Growth Des*, 2021, **21**, 5017–5026.

21 M. Mirjolet, F. Sánchez and J. Fontcuberta, *Adv Funct Mater*, 2019, **29**, 1808432.

22 S. Amoruso, A. Sambri and X. Wang, *J Appl Phys*, 2006, **100**, 013302.

23 A. Ojeda-G-P, M. Döbeli and T. Lippert, *Adv Mater Interfaces*, 2018, **5**, 1701062.

24 H. N. Lee, S. S. Ambrose Seo, W. S. Choi and C. M. Rouleau, *Sci Rep*, 2016, **6**, 19941.

25 J. V. Barth, G. Costantini and K. Kern, *Nature*, 2005, **437**, 671–679.

26 J. Lyu, I. Fina, R. Solanas, J. Fontcuberta and F. Sánchez, *Sci Rep*, 2018, **8**, 495.

27 P. Jiang, Q. Luo, X. Xu, T. Gong, P. Yuan, Y. Wang, Z. Gao, W. Wei, L. Tai and H. Lv, *Adv Electron Mater*, 2021, **7**, 2000728.

28 J. P. B. Silva, K. C. Sekhar, R. F. Negrea, J. L. MacManus-Driscoll and L. Pintilie, *Appl Mater Today*, 2022, **26**, 101394.

29 F. Cüppers, K. Hirai and H. Funakubo, *Nano Converg*, 2022, 9, 56.

30 J. Lyu, I. Fina and F. Sánchez, *Appl Phys Lett*, 2020, **117**, 072901.

31 T. Song, S. Estandía, H. Tan, N. Dix, J. Gàzquez, I. Fina and F. Sánchez, *Adv Electron Mater*, 2021, **8**, 2100420.

Electronic Supplementary Information

Ferroelectric $Hf_{0.5}Zr_{0.5}O_2$ films with improved endurance by low temperature epitaxial growth on seed layers

Tingfeng Song,[a] Romain Bachelet,[b] Guillaume Saint-Girons,[b] Ignasi Fina,[a,*] Florencio Sánchez[a,*]

[a] Institut de Ciència de Materials de Barcelona (ICMAB-CSIC), Campus UAB, Bellaterra 08193, Barcelona, Spain

[b] Univ. Lyon, Ecole Centrale de Lyon, INSA Lyon, Université Claude Bernard Lyon 1, CPE Lyon, CNRS, Institut des Nanotechnologies de Lyon - INL, UMR5270, 69134 Ecully, France.

* ifina@icmab.es, fsanchez@icmab.es

Figure S1 XRD Pole figures

Pole figures (top panels) and ϕ-scans (bottom panels) around asymmetrical o-HZO(-111) and STO(111) reflections of the (a) T_S = 550 °C, (b) T_S = 650 °C, and (c) T_S = 800 °C samples.

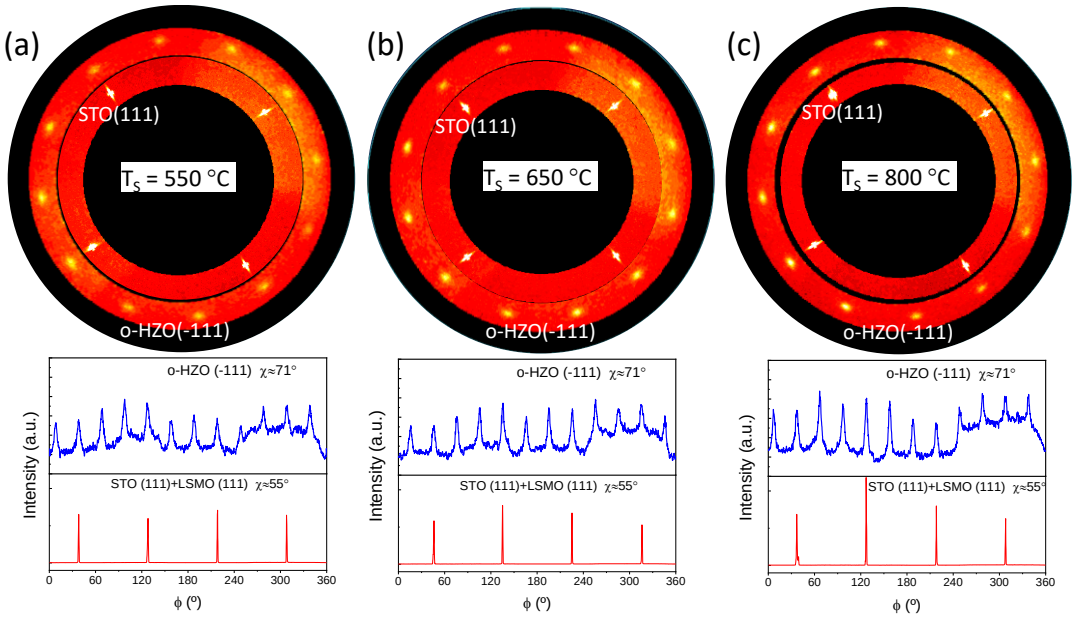

Figure S2 XRD 2θ - χ maps measured with 2D detector

XRD 2θ - χ maps measured around χ = 0° from 2θ = 20° to 50°. The main reflections are indexed at the top. The asterisk mark the position of the m-HZO(-111) reflection in the low T_S films and a Laue frige in the high T_S films.

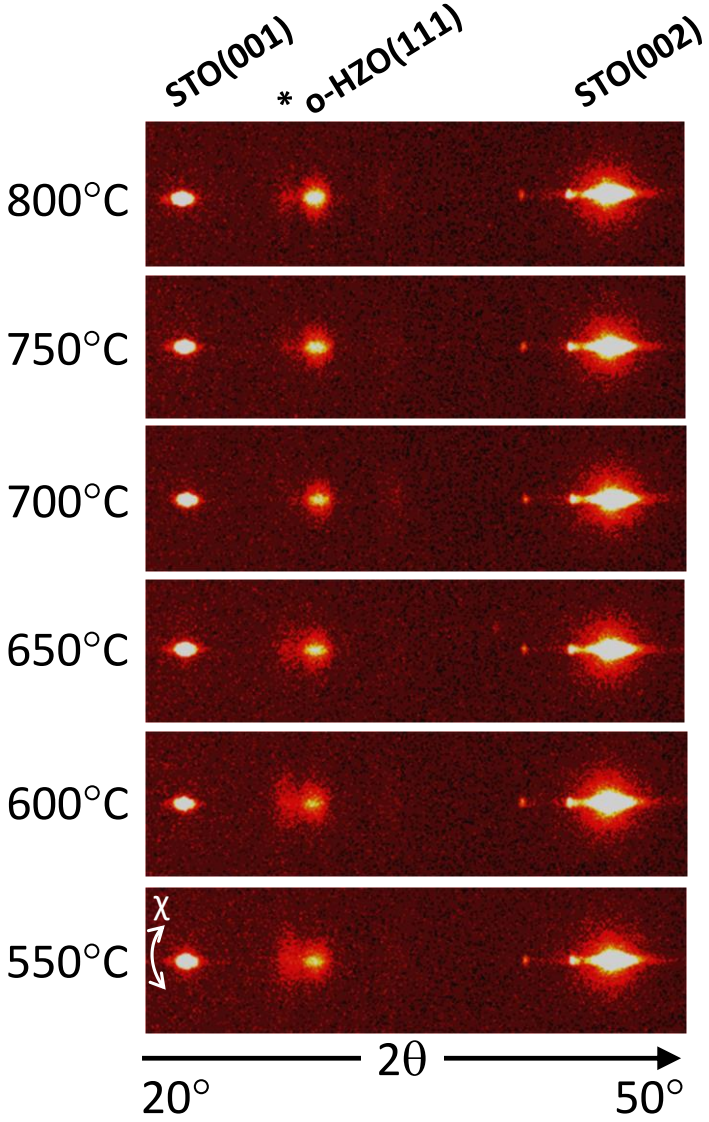

Figure S3 Simulation of Laue fringes

Figure S3 shows the XRD θ-2θ scan of the HZO/LSMO/STO(001) samples. The patterns around the HZO(111) reflections are simulated according the dependence:

$$I(Q) = \left(\frac{\sin\left(\frac{QNc}{2}\right)}{\sin\left(\frac{Qc}{2}\right)}\right)^2$$

where Q = 4πsin(θ)/λ is the reciprocal space vector, N the number of unit cells along the out-of-plane direction and c the corresponding lattice parameter. The simulations (red curves) have been fitted supposing the Nc thickness indicated in each panel.

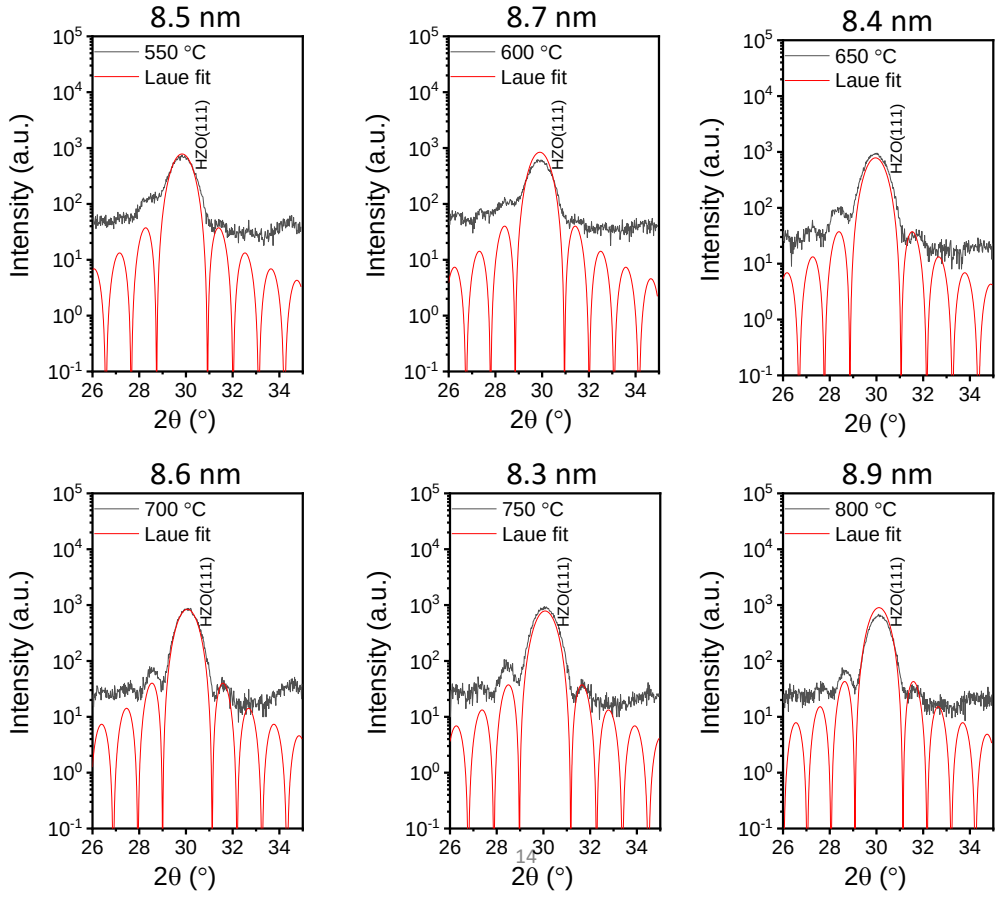

Figure S4 XRD θ-2θ scans of HZO films deposited on Si(001)

XRD θ-2θ scans of HZO films deposited on Si(001) at the temperature indicated on the right. Scans are shifted vertically for clarity. The enlarged 2θ region shown in the right panel was scanned with a longer acquisition time. The dashed vertical line marks the position of the peak in the T_S = 750 °C sample.

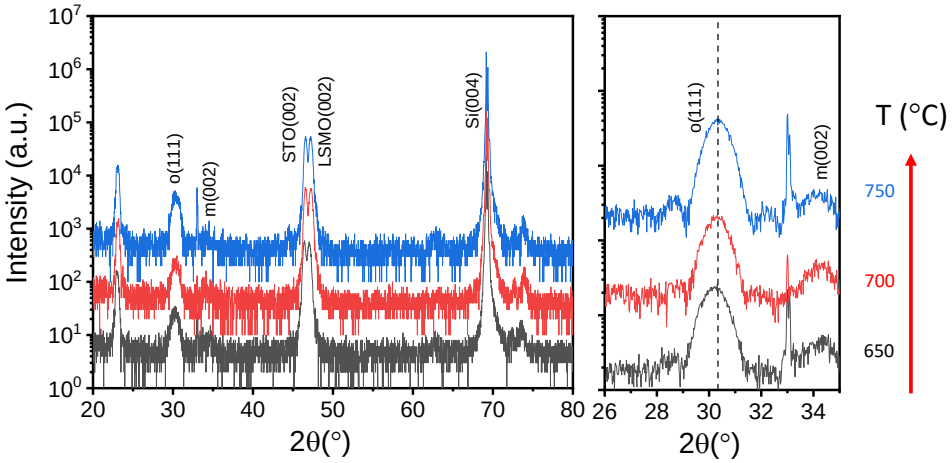

Figure S5 Current-voltage loops measured in the HZO films deposited on STO(001)

Current-voltage loops measured in the HZO films deposited on STO(001) at the temperature indicated in the bottom right. Polarization loops shown in Figure 3a were obtained by integration of these current - voltage loops.

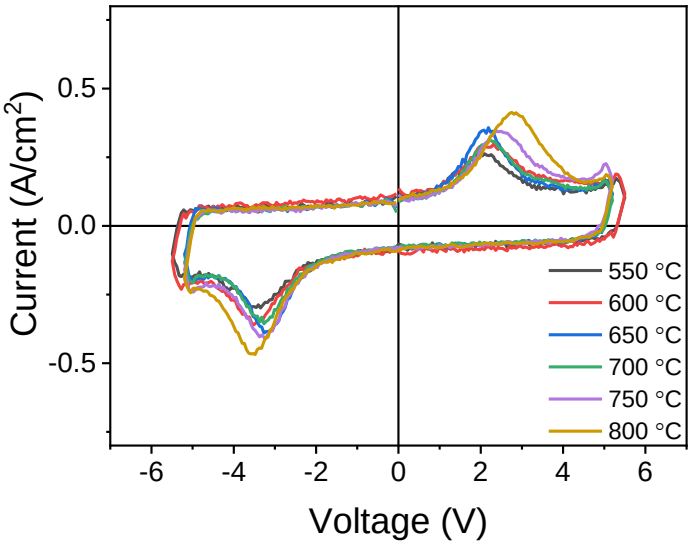

Figure S6 Current - voltage and corresponding polarization - voltage loops of the HZO films deposited on Si(001)

Current - voltage (a) and corresponding polarization - voltage (b) loops of the HZO films deposited on Si(001) at the temperature indicated in the bottom right.

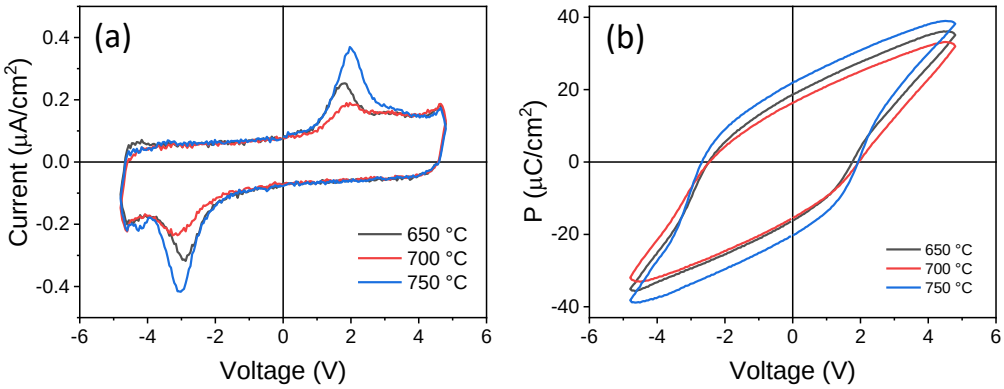

Figure S7 PUND measurements

In Figure S7(a), the PUND loops measured with 1 s delay time for all the studied samples are shown. Similar Pr values are obtained. In Figure S7(b), a comparison of the loops obtained with dynamic and PUND methods for a representative sample (T_s = 750 °C) is shown. It can be observed that the coercive field is larger for the PUND loop. This results from the presence of the fluid imprint field [1]. The increase of coercive field does not allow to fully saturate the polarization of the sample at the used maximum applied electric field. Larger electric field results on device breakdown. In Figure S7(c), it can be observed that the P_r obtained using PUND is slightly less than those obtained by dynamic method. In both cases the trend is the same indicating that the decrease of polarization while decreasing T_S is small.

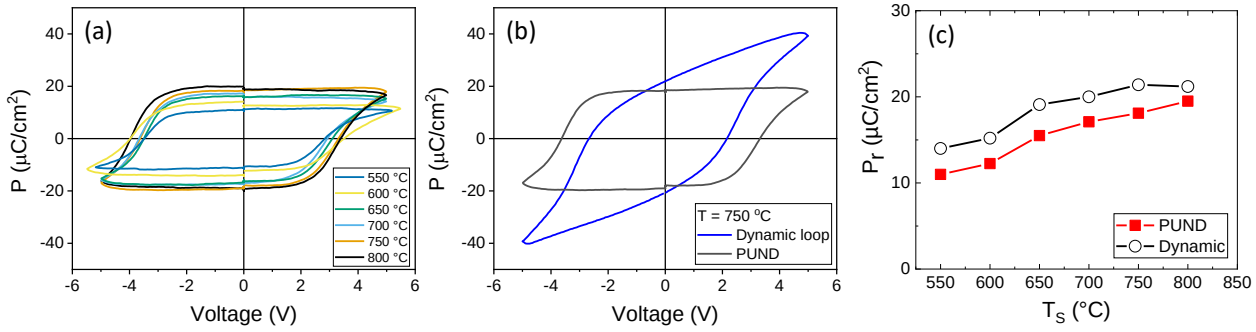

Figure S8 Polarization – voltage loops measured in the pristine state and after the indicated number of cycles

Polarization – voltage loops measured in the pristine state and after the indicated number of cycles (indicated at the bottom right in each panel) for films on STO(001) deposited at the temperature indicated in the top right of each panel. Loops are a selection of the measured to plot the endurance graphs shown in Figures 4 a-f.

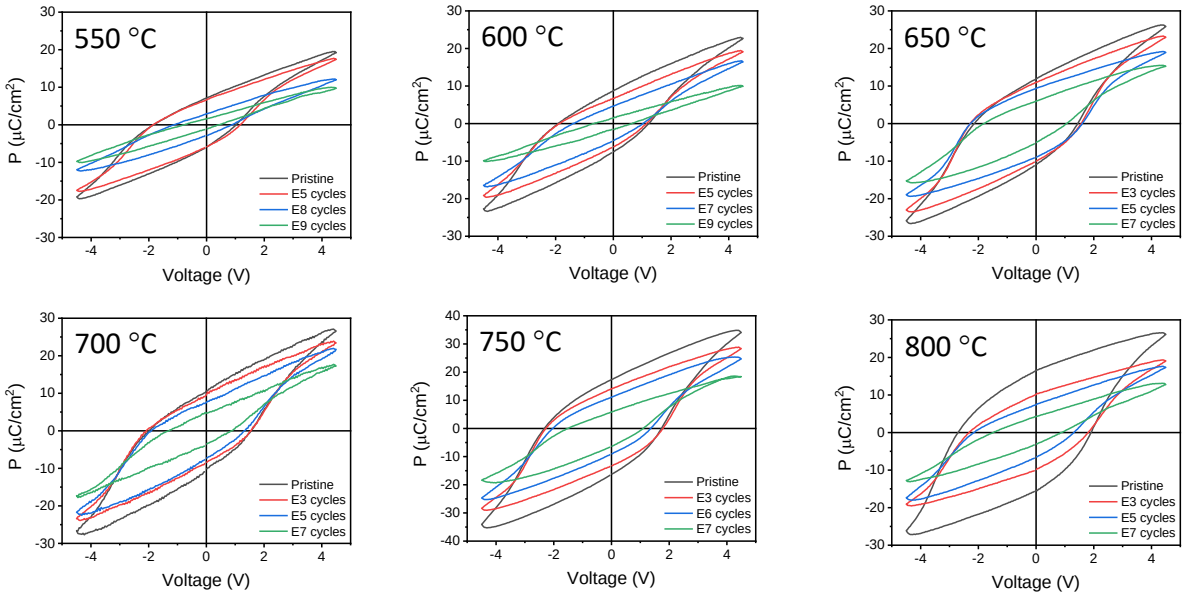

Figure S9 Polarization retention measurements for films on STO(001)

Polarization retention measurements at for positive (blue squares) and negative (red circles) poling of 4.5 V for films on STO(001) deposited at the temperature indicated in the top right of each panel. Lines are fits to $P_r = P_0 \cdot \tau_d^{-n}$ equation.

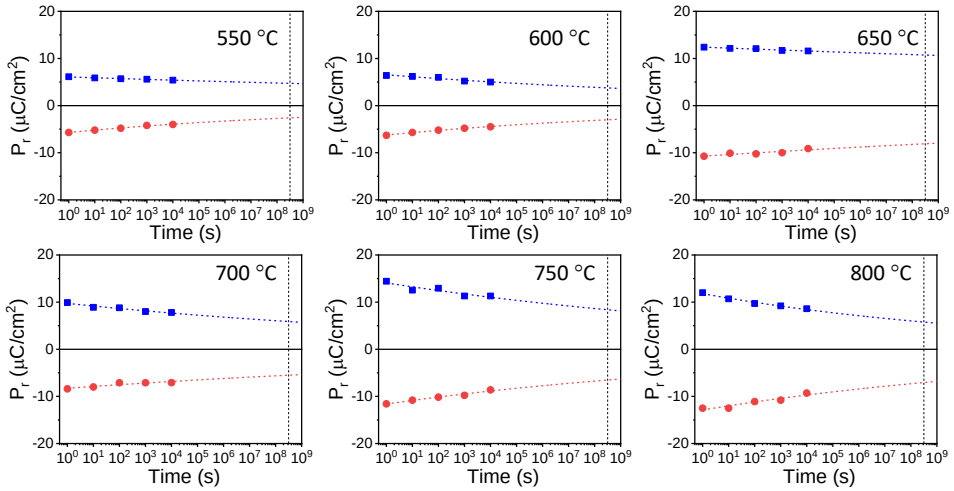

Figure S10 Leakage current curves measured in the pristine state and after the indicated number of cycles

Leakage current curves measured in the pristine state and after the indicated number of cycles (indicated at the bottom left in each panel) for films on STO(001) deposited at the temperature indicated in the bottom right of each panel. Figure 5 is plotted from leakage data at -1 and +1 V in these curves.

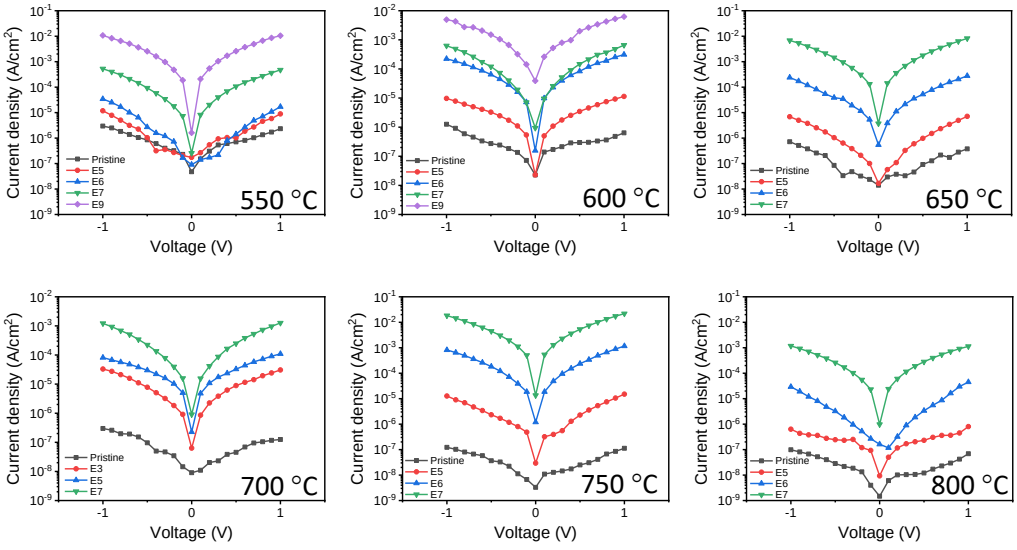

Reference

1 P. Buragohain, A. Erickson, P. Kariuki, T. Mittmann, C. Richter, P. D. Lomenzo, H. Lu, T. Schenk, T. Mikolajick, U. Schroeder and A. Gruverman, *ACS Appl Mater Interfaces*, 2019, **11**, 35115–35121.

ARTICLE

Ferroelectric $Hf_{0.5}Zr_{0.5}O_2$ films with improved endurance by low temperature epitaxial growth on seed layers †

Received 00th January 20xx,
Accepted 00th January 20xx

DOI: 10.1039/x0xx00000x

Tingfeng Song,[a] Romain Bachelet,[b] Guillaume Saint-Girons,[b] Ignasi Fina,*[a] and Florencio Sánchez*[a]

The crystallization temperature is a critical parameter in the stabilization of the metastable ferroelectric phase of HfO_2. The optimal crystallization temperature used for polycrystalline films is too low to grow epitaxial films. We have developed a new growth strategy, based on the use of an ultrathin seed layer, to obtain high-quality epitaxial films of orthorhombic $Hf_{0.5}Zr_{0.5}O_2$ at lower temperature. The threshold temperature for epitaxy is reduced from about 750 °C to about 550 °C by using a seed layer. Epitaxial films deposited at low temperature exhibit highly enhanced endurance, and films grown at 550 - 600 °C have high polarization, no wake-up effect, and greatly reduced fatigue and improved endurance in comparison with the films deposited at high temperature without a seed layer. We propose that the endurance enhancement is due to a positive effect of the defects, which limit the propagation of pinned ferroelectric domains.

1. Introduction

HfO_2 films can exhibit robust ferroelectricity at room temperature, and their compatibility with CMOS processes opens up new possibilities for memories and other ferroelectrics-based devices [1,2]. Bulk HfO_2 under ambient conditions is monoclinic and paraelectric. Ferroelectricity arises in a metastable orthorhombic phase stabilized in HfO_2 nanometric films, typically doped, and prepared under particular conditions. In the commonly investigated polycrystalline films, the orthorhombic phase is formed by thermal annealing. Annealing at excessively high temperature [3,4] or with excessively long time [5] promotes the formation of the stable monoclinic phase. It is proposed that the stabilization of the metastable ferroelectric phase is due to a combined effect of the surface energy contribution and kinetic limitations [6]. Before annealing, the quasi-amorphous films would have small orthorhombic nuclei. During annealing, the nanocrystals transform to tetragonal phase that is stable at high temperature. However, when the crystal grains increase in size, the lowest energy corresponds to the monoclinic phase. However, the energy barrier for this phase transformation is high, and the transformation is kinetically suppressed in $Hf_{0.5}Zr_{0.5}O_2$ (HZO) films if annealing is short and at moderate temperature. It has also been reported that monoclinic phase can be transformed to tetragonal and orthorhombic phases by very high temperature annealing (1000 - 1200 °C) in solid phase epitaxy of Y-doped HfO_2 films [7]. Therefore, in crystallization of quasi-amorphous films, annealing temperature is a critical parameter to stabilize the metastable orthorhombic phase rather than the thermodynamically stable monoclinic phase.

Epitaxial growth from a vapor phase radically differs from crystallization processes by annealing. Diffusion of atoms on a surface and chemical bonding at specific positions generally requires high thermal energy, suitable saturation conditions, and a growth rate low enough to limit crystalline defects. In particular, the ferroelectric phase of doped HfO_2 has been stabilized in epitaxial films, mainly by pulsed laser deposition, and with substrate temperature around 700-800 °C [8–12]. The study of the window for epitaxial growth of ferroelectric HZO films revealed a severe reduction in crystallinity for temperature (substrate heater block) below around 700 °C [13]. The possibility of epitaxial growth at lower temperature would be desirable due to its impact on the microstructure of the film. Epitaxial films of ferroelectric HfO_2 generally present mixture of phases and crystal variants. Microstructure, including polymorphs ratio, crystal grain size and defects, can be critical in the ferroelectric properties of HfO_2. However, the high thermal energy required for epitaxy precludes investigating low-temperature conditions that could influence the stabilization of the orthorhombic phase and tailor the microstructure of the films.

In the heteroepitaxial growth, the interface energy is an important factor in the formation of crystal nuclei and in determining the crystal polymorphs that nucleate. We have investigated a new strategy to grow ferroelectric HfO_2 films, with the aim of widening the window for epitaxial growth at

[a] Institut de Ciència de Materials de Barcelona (ICMAB-CSIC), Campus UAB, Bellaterra 08193, Barcelona, Spain. E-mail: ifina@icmab.es, fsanchez@icmab.es
[b] Univ. Lyon, Ecole Centrale de Lyon, INSA Lyon, Université Claude Bernard Lyon 1, CPE Lyon, CNRS, Institut des Nanotechnologies de Lyon - INL, UMR5270, 69134 Ecully, France.

†Electronic Supplementary Information (ESI) available: XRD Pole figures. XRD 2θ - χ maps measured with 2D detector. Simulation of Laue fringes. XRD θ-2θ scans of HZO films deposited on Si(001). Current-voltage loops measured in the HZO films deposited on STO(001). Current - voltage and corresponding polarization - voltage loops of the HZO films deposited on Si(001). PUND measurements. Polarization – voltage loops measured in the pristine state and after the indicated number of cycles. Polarization retention measurements for films on STO(001). Leakage current curves measured in the pristine state and after the indicated number of cycles. See DOI: 10.1039/x0xx00000x

lower temperature. Films were grown in two steps. In the first step, an ultra-thin seed layer is grown at optimal high temperature (800 °C) for heteroepitaxial growth of HZO [9–13]. The HZO growth then continues (second step) at a lower temperature on the epitaxial HZO seed layer. Homoepitaxial growth is expected to be possible at lower temperature, since there is not a HZO film / HZO seed layer interface energy contribution, in contrast with the high interface energy at the HZO seed layer / substrate interface. We will show that the use of the seed layer allows the stabilization of the orthorhombic phase at a lower temperature. The films grown at low temperature (550 - 600 °C) show excellent ferroelectric properties: slightly reduced ferroelectric polarization, absence of wake-up effect and greatly enhanced robustness against fatigue.

2. Experimental

Top ferroelectric HZO films and bottom $La_{0.67}Sr_{0.33}MnO_3$ (LSMO) electrodes were grown on (001)-oriented $SrTiO_3$ (STO) substrates in a single process by pulsed laser deposition (PLD) using a KrF excimer laser (248 nm wavelength). The LSMO electrodes, thickness t ~ 25 nm, were grown at T_S = 700 °C and oxygen pressure P_{O2} = 0.1 mbar. HZO films were then grown in two steps. First, an ultra-thin (t ~ 2.2 nm) HZO seed layer was grown at 800 °C and 0.1 mbar of oxygen with 200 laser pulses at a growth rate of 0.11 Å/laser pulse. Next, the seed layer was cooled under 0.1 mbar of oxygen to a temperature T_S in the 550 - 750 °C range, and a HZO film (t ~ 6.6 nm) was grown with 600 laser pulses at that temperature and same oxygen pressure and growth rate that the seed layer. Another film was grown at 800 °C, in a two steps process with a dwell time of 18 min after deposition of the first 2.2 nm. At the end of the deposition, samples were cooled under 0.2 mbar of oxygen partial pressure. Another series of films was deposited at 650, 700 and 750 °C on Si(001) buffered with an epitaxial STO layer. Details on STO growth conditions and structural properties are reported elsewhere [14,15].

Structural characterization of the HZO films was performed by X-ray diffraction (XRD) using Cu Kα radiation. Platinum top electrodes, 20 nm thick and 20 µm in diameter, were grown by dc magnetron sputtering through stencil masks for electrical characterization. Ferroelectric polarization loops were measured at 1 kHz using the dynamic leakage current compensation (DLCC) procedure at room temperature in top-bottom configuration [16,17]. Endurance was measured cycling the sample at 100 kHz using bipolar square pulses of amplitude of 4.5 V and measuring polarization loops at 1 kHz.

3. Results

Fig. 1a shows XRD θ-2θ scans of the HZO films on STO substrates. The growth temperature (second step) is indicated on the right. The high intensity peaks at 2θ around 23 and 47° correspond to the (001) and (002) reflections from the STO substrate. The corresponding reflections from the LSMO electrode lie to the right of the substrate peaks. Furthermore, all samples exhibit a peak at 2θ around 30°, the position of the (111) reflection of the orthorhombic (o) phase of HZO. Therefore, HZO crystallizes over the entire investigated T_S range. The peak is broad, as expected considering that the HZO total thickness is less than 9 nm. Epitaxial stabilization of the ferroelectric phase of HZO on LSMO electrodes usually requires deposition temperature above around 700 °C [9–13,18]. Pole figures (Fig. 1c) and ϕ-scans (Fig. 1c) around asymmetrical o-HZO(-111) reflections confirm that the film grows epitaxially, even at T_S = 550 °C is epitaxial (pole figures of the T_S = 650 °C and 800 °C samples are in Supporting Information S1). The films show the epitaxial relationship and four sets of crystal variants usual in the epitaxial growth on LSMO(001) [9]. The right panel in Fig. 1a shows a 2θ zoomed region around the o-HZO(111) reflection, measured with a longer acquisition time. The o-HZO(111) reflection from all the films is accompanied by Laue fringes, more pronounced in the films deposited at higher temperature, indicating better crystalline quality and flatter interfaces. XRD measurements with a 2D detector are shown in Supporting Information S2. The o-HZO(111) reflection is a bright spot in all the samples, without broadening along the χ angle. There is an additional Bragg spot at around 2θ = 28.5° in the T_S = 550 °C film. The 2θ position and the elongation along χ indicates that corresponds to the monoclinic (m) HZO(-111) reflection [9,13]. The m-HZO(-111) spot decreases in intensity with T_S increasing, and it is not detected in the films deposited at T_S higher than 650 °C. In the films deposited at the highest T_S, 750 and 800 °C, the sharp spot at a close position is a Laue fringe of the o-HZO(111) reflection. The total thickness of the HZO stack (seed layer and film) in each sample was determined by

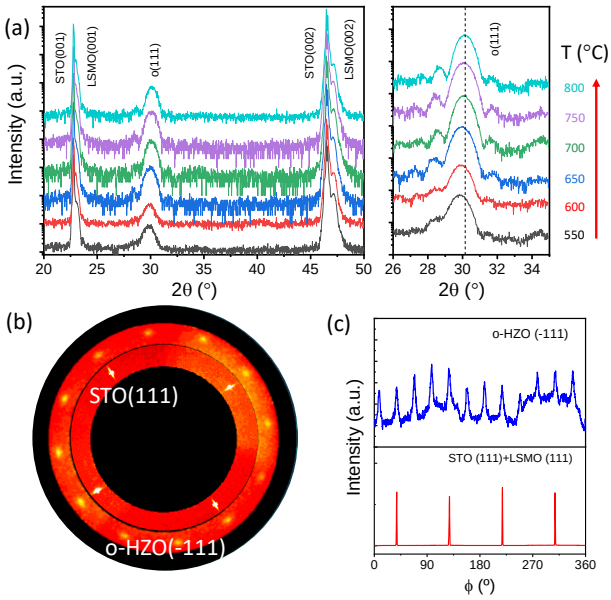

Fig. 1 (a) XRD θ-2θ scans of HZO films deposited on STO(001) at the temperature indicated on the right. Scans are shifted vertically for clarity. The enlarged 2θ region shown in the right panel was scanned with a longer acquisition time. The dashed vertical line marks the position of the peak in the T_S = 800 °C sample. (b) Pole figures and (c) ϕ-scans around o-HZO(-111) and STO(111) reflections of the T_S = 550 °C sample.

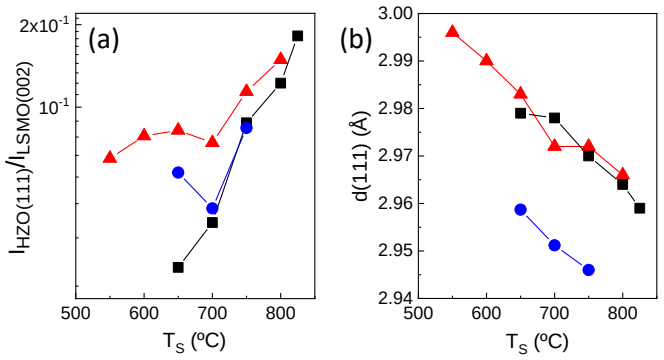

Fig. 2 Intensity of the o-(111) reflection, normalized to that of the LSMO(002) peak (a), and out-of-plane lattice distance corresponding to the o-(111) reflection (b), as a function of deposition temperature T_S for films on STO(001) (red triangles) and Si(001) (blue circles). Black squares are data corresponding to films on STO(001) deposited without a seed layer [13].

simulation of o-HZO(111) reflection and the Laue fringes (Supporting Information S3). The total HZO thickness in the series of samples ranges from 8.3 to 8.9 nm, in agreement with the expected HZO growth rate of 0.11 Å/laser pulse. In Fig. 1, a tiny peak around 34.5°, is also barely observed, corresponding to the position of the HZO{002} reflections of the monoclinic (m) phase. The peak, of very low intensity, is observed only in some films, without correlation with T_S. In contrast, the position of the o-HZO(111) peak varies monotonically with the deposition temperature. The dashed vertical line marks the position of the peak for the T_S = 800 °C sample. It can be seen that as T_S decreases, the peak shifts to a lower angle, indicating that the HZO(111) out-of-plane lattice distance, d(111), increases. To demonstrate that a seed layer is also effective for low-temperature epitaxy on Si(001) substrates, we used epitaxial STO buffer layers, which allow epitaxial growth of LSMO electrodes and HZO ferroelectric films [14]. XRD θ-2θ scans of three films grown at 550, 600 and 650 °C (Supporting Information S4) confirm stabilization of the orthorhombic phase at low T_S, with a similar d(111) - T_S dependence than the films on STO(001).

The intensity of the o-HZO(111) diffraction peak can be used as an approximation to estimate the orthorhombic phase content in the films. Fig. 2(a) shows the intensity of the o-HZO(111) peak, normalized to the LSMO(002) peak to compensate potential differences in the XRD measurement conditions of the samples, of films grown on seed layers on STO (red triangles) and Si (blue circles) substrates. The normalized intensity of the films on STO decreases with lowering T_S to 700 °C, and shows less dependence for T_S between 700 and 550 °C. The intensity-T_S dependence is similar in the three samples on Si, although the normalized intensity is lower. The graph also includes the corresponding normalized intensity of films deposited at various T_S directly on LSMO/STO(001) electrode, without a seed layer (black squares), and having the same total thickness (~8.8 nm) [13]. The T_S = 800 °C sample with seed layer has slightly higher normalized intensity than the corresponding film without seed layer, which could be caused by the 18 min dwell time. The intensity of the films grown without seed layer decreases very sharply with T_S, and is very low for T_S below 750 °C. Fig.2(a) indicates that i) the growth of highly crystalline films below 750 °C is only achieved on seed layers and, ii) for higher temperatures, the use of a seed layer enhances HZO crystallization.

The variation of the position of the o-HZO(111) peak with T_S (Figure 1) is quantified in Fig. 2(b). The lattice parameter d(111) increases monotonically with decreasing T_S (red triangles) to about 1.3%, and matches that of films grown at the same temperature without a seed layer (black squares). The unit cell expansion of a film grown by PLD can be caused by defects that form when the energy of the PLD plasma is high [19–21]. The energy of the atomic species in the PLD plasma reaching the substrate depends on the laser fluence, the target - substrate distance and the gas pressure [22–24]. These parameters were kept constant in the preparation of the films discussed here. However, the number of defects that form in a film depends on the balance between growth kinetics and thermodynamics [25]. This balance, as demonstrated recently in the epitaxial growth of $BaTiO_3$ films, can be tailored by the substrate temperature [26]. The damage caused by the energetic PLD plasma is reduced by the high thermal energy in HZO films grown at high T_S, while lowering T_S thermal energy is less, leading to more defects and d(111) expansion. The films on Si show the same dependence of d(111) on T_S, but with a reduced value compared to the equivalent films on STO, which is a consequence of the tensile stress caused by the mismatch between thermal expansion

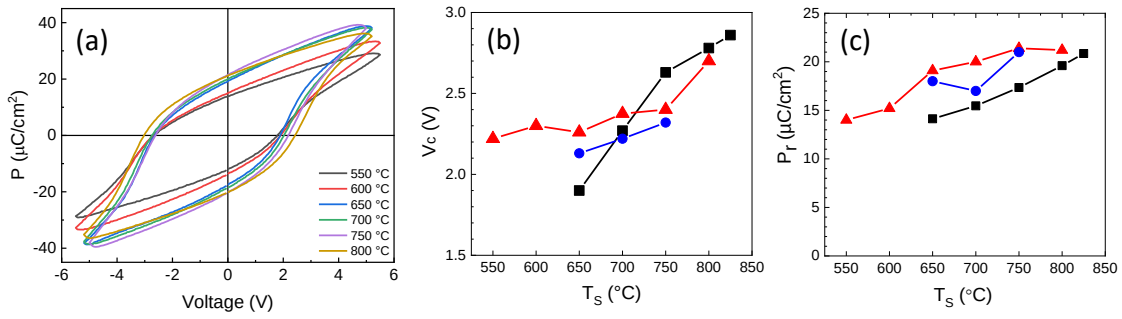

Fig. 3 (a) Ferroelectric polarization loops of HZO films deposited at the temperature indicated at the bottom right. Coercive voltage (b) and remanent polarization (c), as a function of deposition temperature T_S for films on STO(001) (red triangles) and Si(001) (blue circles). Black squares are data corresponding to films on STO(001) deposited without a seed layer [11].

coefficients (TEC) of HZO and Si. Although TEC mismatch effects are less relevant if T_S is lower, the two lineal dependences are parallel, probably because the seed layer is grown in all samples at T_S = 800 °C.

All films are ferroelectric, confirming the stabilization of the orthorhombic phase throughout the T_S range. The polarization loops of the films on STO(001) (Fig. 3(a), with the corresponding current-voltage loops in Supporting Information S5) are shifted towards negative voltage values. The positive coercive voltage V_{C+} increases with T_S from around 1.8 V to 2.4 V, while the negative coercive voltage V_{C-} ranges from -2.7 V to -3.0 V. It can be observed that all the loops are shifted towards the left between 0.45 and 0.90 V. This indicates that in all samples the imprint electric field is towards the LSMO electrode. The average coercive voltage $V_C = (V_{C+} + |V_{C-}|)/2$ is in the range of 2.2 - 2.7 V, increasing with T_S (Figure 3b, red triangles), corresponding to coercive electric field E_C in the 2.5 - 3.1 MV/cm range. The coercive voltage of the three films grown on Si substrate is slightly lower and shows a similar T_S dependence (blue circles). Epitaxial films grown directly on LSMO/STO(001) without a seed layer exhibit similar V_C values and T_S dependence (black squares). High E_C of about 2.5 - 3 MV/cm, which exceeds the usual E_C of polycrystalline films, is common in HZO epitaxial films of similar thickness [11,13]. The remanent polarization is plotted against T_S in Fig. 3(c) (red triangles). P_r decreases moderately with decreasing growth temperature, from 21.2 μC/cm² in the T_S = 800 °C film to 14 μC/cm² in the T_S = 550 °C film. Similar trend is observed if P_r values are obtained from PUND measurements Supporting Information S7). The remanent polarization of the films on Si (polarization loops shown in Supporting Information S6) is comparable (blue circles). In the films deposited without seed layer, the

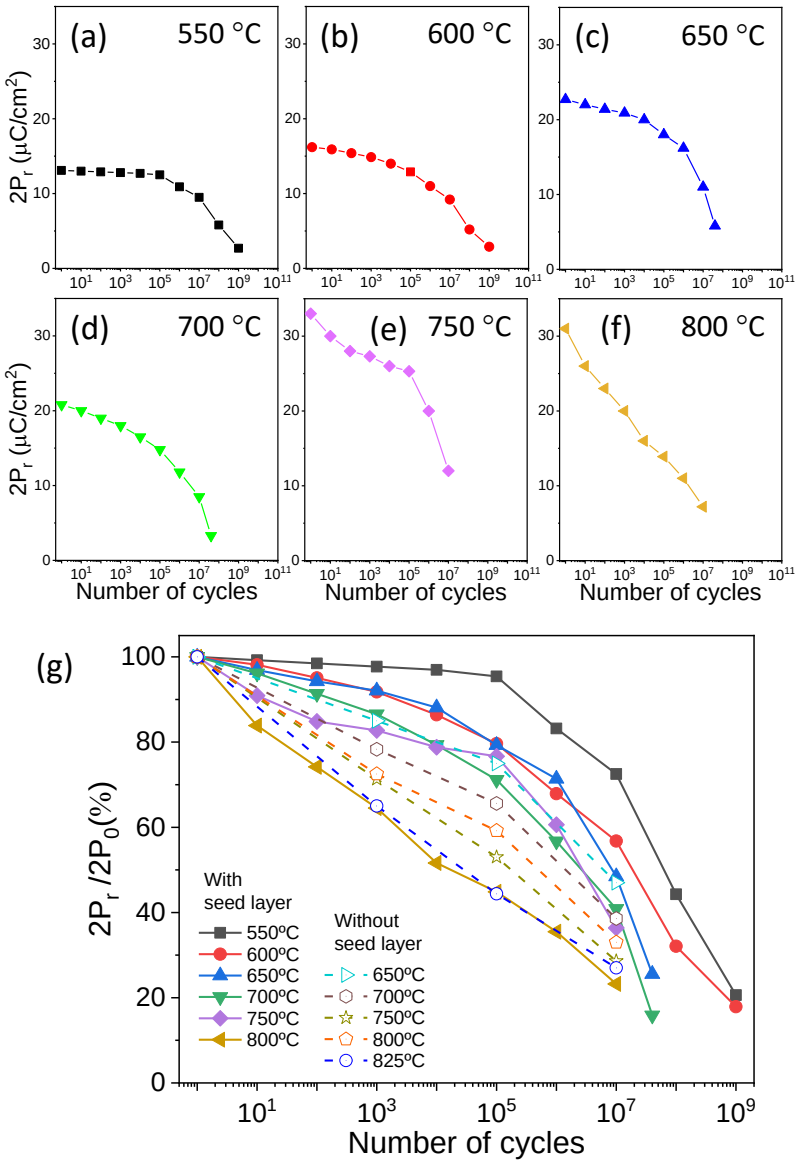

Fig. 4 Endurance, measured with bipolar rectangular pulses of frequency 100 kHz and amplitude 4.5 V, of T_S = 550 °C (a), 600 °C (b), 650 °C (c), 700 °C (d), 750 °C (e), and 800 °C (f) films on STO. (g) Comparison of endurance (remanent polarization is normalized to the pristine state value) of the films grown at various T_S on a seed layer (solid symbols and solid lines) films grown at various T_S without a seed layer (empty symbols and dashed lines). Data of films grown without a seed layer are reported in [24].

polarization is similar in the film deposited at 800 °C, 19.6 μC/cm², but decreases sharply with T_S to around 14 μC/cm² in the T_S = 650 °C film.

Fatigue was investigated by cycling the capacitors with bipolar rectangular pulses of frequency 100 kHz and amplitude 4.5 V, close to the voltage used to obtain saturated loops (Fig. 3(a)). Endurance measurements are shown in Fig. 4(a-f) (see Supporting Information S8 for polarization loops). There is no wake-up effect in these epitaxial capacitors. Wake-up effect is usually pronounced in polycrystalline films, and it proposed to be caused by oxygen vacancies redistribution or electric-field induced phase transformations [2,27]. Epitaxial films of doped HfO_2 typically are wake-up free, or a very low wake-up effect [9,28,29] which can be due to the lower amount of defects in epitaxial films. The T_S = 550 °C film (Fig. 4(a)) has a moderately low $2P_r$ of 13.1 μC/cm² in the pristine state, and there is no significant fatigue over 10^5 cycles ($2P_r$ = 12.5 μC/cm²). $2P_r$ drops to 9.5 μC/cm² after 10^7 cycles, and after 10^9 it is only 2.7 μC/cm². More cycles caused electric breakdown. HZO films grown at higher temperature show fatigue from the beginning, the greater the higher T_S. In the T_S = 600 °C sample (Fig. 4(b)) the decrease in $2P_r$ after 10^5 cycles is low, decreasing from 16.2 to 12.9 μC/cm². Thereafter, fatigue is more pronounced and $2P_r$ is 2.9 μC/cm² after 10^9 cycles, before breakdown occurs. In the T_S = 650 and 700 °C samples (Fig. 4(c, d), respectively), $2P_r$ in the pristine state is greater than 20 μC/cm², but high fatigue begins after fewer cycles and, moreover, breakdown occurs earlier, after 4x10^7 cycles. In the samples grown at the highest temperatures, 750 and 800 °C (Fig. 4(e, f), respectively), with high initial $2P_r$ of more than 30 μC/cm², the degradation of polarization is more evident, and the tendency of early breakdown with increased T_S is confirmed, occurring after 10^7 cycles in both films. Therefore, the films deposited at low temperature, although they have lower polarization in the pristine state, are less affected by fatigue and more robust against breakdown. The polarization is normalized in Fig. 4(g) to compare the endurance of the films grown at various T_S on a seed layer (solid symbols and solid lines). The robustness against fatigue and electrical breakdown at low T_S is evident. The graph also includes data from films grown at various T_S without a seed layer (empty symbols and dashed lines) [30]. The films deposited at low T_S without seed layer already showed less fatigue. However, the crystallization and ferroelectric polarization of films deposited at less than 700 °C was too low. The use of a seed layer, which enhances crystallization, allows for epitaxial growth and high polarization at lower temperature, with a positive impact on fatigue and resistance against breakdown as shown in Fig. 4(g). Moreover, all films in the series show excellent retention, with extrapolated remanent polarization after 10 years above 47% of the initial value for either positive or negative poling (Supporting Information S9).

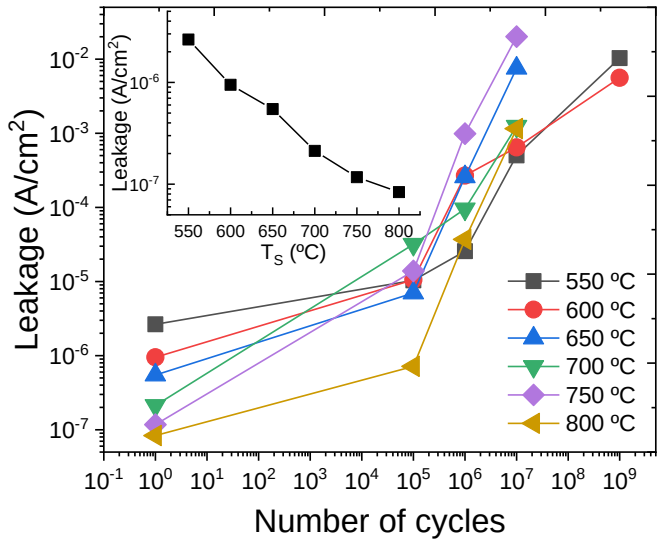

Fig. 5 Evolution of current leakage density with the number of cycles of the films on STO(001) deposited at the temperature indicated at the bottom right. Inset: Pristine state leakage current density of films on STO(001) as a function of deposition temperature.

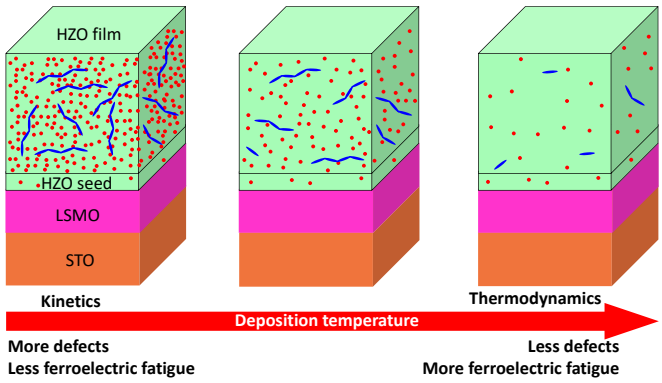

Fig. 6 Schematics of the expected amount of point (red color) and extended (blue color) defects as a function of the deposition temperature.

It has been shown here that using a HZO seed layer, in comparison with films without it, allows enhancing crystalline quality, polarization and resistance against fatigue of ferroelectric HZO films. Also, it has been shown that lowering the growth temperature results in less polarization but also less fatigue. The decrease in polarization is a consequence of the reduced crystallization and the lower amount of orthorhombic phase in films deposited at low T_S. Furthermore, there is a greater expansion of the out-of-plane lattice parameter with decreasing T_S, indicating a higher density of point defects. Domain pinning at point defects is a possible mechanism of fatigue, but the lower fatigue in low T_S films suggests that this is not a primary fatigue mechanism in epitaxial films. On the other hand, low T_S films are less crystalline and may have extended defects. The higher number of point and extended defects in low-temperature deposited films probably causes the monotonic increase of leakage current in pristine state with decreasing deposition temperature (Fig. 5, inset). Leakage (see Supporting Information S10 for leakage curves) increases with cycling in all samples, particularly after 10^5 - 10^6 cycles, but the increase in low T_S films is less and, after 10^7 cycles, the T_S = 550 and 600 °C films have the lowest leakage. This may contribute to the high robustness of low T_S films against electrical breakdown. Therefore, point and extended defects in films grown at low temperature (Fig. 6) do not negatively affect

endurance and, on the contrary, may be a major factor for lower fatigue. We recently showed that parasitic monoclinic phase has a positive effect on endurance, with less fatigue in films on STO substrates with coexisting orthorhombic and monoclinic phases than in almost pure orthorhombic films on scandate substrates [31]. We argued that this is a consequence of the suppression of propagation of pinned domains at the boundaries with the non-ferroelectric phase. Here, in films grown at lower temperature, a greater amount of monoclinic phase, extended defects and more defective grain boundaries between orthorhombic and monoclinic phases could help to suppress the rapid propagation of pinned domains.

4. Conclusions

In conclusion, the use of a seed layer allows the epitaxial growth of enhanced ferroelectric HZO films on STO(001) and Si(001) at significantly lower temperature. The orthorhombic phase forms over a wide temperature range, with the (111) out-of-plane lattice parameter decreasing linearly with deposition temperature by about 1.3%. The crystallization of the orthorhombic phase is reduced with decreasing substrate temperature and the polarization is slightly reduced. However, the films grown at low temperature are more robust against ferroelectric fatigue and electrical breakdown. The results suggest that the pinning of ferroelectric domains at point defects is not a major mechanism of fatigue. The suppression of pinned domain propagation at more defective regions and grain boundaries in low-temperature deposited films is proposed as the reason of the enhancement.

Conflicts of interest

There are no conflicts to declare.

Acknowledgements

Financial support from the Spanish Ministry of Science and Innovation (MCIN/AEI/ 10.13039/501100011033), through the Severo Ochoa FUNFUTURE (CEX2019-000917-S), PID2020-112548RB-I00 and PID2019-107727RB-I00 projects, and from CSIC through the i-LINK (LINKA20338) program is acknowledged. We also acknowledge project TED2021-130453B-C21, funded by MCIN/AEI/10.13039/501100011033 and European Union NextGeneration EU/PRTR. TS is financially supported by China Scholarship Council (CSC) with No. 201807000104. TS work has been done as a part of his Ph.D. program in Materials Science at Universitat Autònoma de Barcelona. RB and GSG acknowledge financial support from the French national research agency (ANR) through the projects DIAMWAFEL (No. ANR-15-CE08-0034), LILIT (No. ANR-16-CE24-0022), and MITO (No. ANR-17-CE05-0018), as well as P. Regreny, C. Botella, and J. B. Goure for the technical support.

References

1 K. Sun, J. Chen and X. Yan, *Adv Funct Mater*, 2021, **31**, 2006773.

2 M. H. Park, Y. H. Lee, T. Mikolajick, U. Schroeder and C. S. Hwang, *MRS Commun*, 2018, **8**, 795–808.

3 M. Hyuk Park, H. Joon Kim, Y. Jin Kim, W. Lee, T. Moon and C. Seong Hwang, *Appl Phys Lett*, 2013, **102**, 242905.

4 H. A. Hsain, Y. Lee, G. Parsons and J. L. Jones, *Appl Phys Lett*, 2020, **116**, 192901.

5 J. Wang, D. Zhou, W. Dong, Y. Yao, N. Sun, F. Ali, X. Hou and F. Liu, *Adv Electron Mater*, 2021, **7**, 2000585.

6 M. H. Park, Y. H. Lee, T. Mikolajick, U. Schroeder and C. S. Hwang, *Adv Electron Mater*, 2019, **5**, 1800522.

7 Y. Tashiro, T. Shimizu, T. Mimura and H. Funakubo, *ACS Appl Electron Mater*, 2021, **3**, 3123–3130.

8 T. Shimizu, K. Katayama, T. Kiguchi, A. Akama, T. J. Konno, O. Sakata and H. Funakubo, *Sci Rep*, 2016, **6**, 32931.

9 J. Lyu, I. Fina, R. Solanas, J. Fontcuberta and F. Sánchez, *Appl Phys Lett*, 2018, **113**, 082902.

10 P. Nukala, Y. Wei, V. de Haas, Q. Guo, J. Antoja-Lleonart and B. Noheda, *Ferroelectrics*, 2020, **569**, 148–163.

11 I. Fina and F. Sánchez, *ACS Appl Electron Mater*, 2021, **3**, 1530–1549.

12 Y. Wang, Q. Wang, J. Zhao, T. Niermann, Y. Liu, L. Dai, K. Zheng, Y. Sun, Y. Zhang, J. Schwarzkopf, T. Schroeder, Z. Jiang, W. Ren and G. Niu, *Appl Mater Today*, 2022, **29**, 101587.

13 J. Lyu, I. Fina, R. Solanas, J. Fontcuberta and F. Sánchez, *ACS Appl Electron Mater*, 2019, **1**, 220–228.

14 J. Lyu, I. Fina, R. Bachelet, G. Saint-Girons, S. Estandía, J. Gázquez, J. Fontcuberta and F. Sánchez, *Appl Phys Lett*, 2019, **114**, 222901.

15 G. Saint-Girons, R. Bachelet, R. Moalla, B. Meunier, L. Louahadj, B. Canut, A. Carretero-Genevrier, J. Gazquez, P. Regreny, C. Botella, J. Penuelas, M. G. Silly, F. Sirotti and G. Grenet, *Chemistry of Materials*, 2016, **28**, 5347–5355.

16 I. Fina, L. Fàbrega, E. Langenberg, X. Martí, F. Sánchez, M. Varela and J. Fontcuberta, *J Appl Phys*, 2011, **109**, 074105.

17 R. Meyer, R. Waser, K. Prume, T. Schmitz and S. Tiedke, *Appl Phys Lett*, 2005, **86**, 142907.

18 H. Y. Yoong, H. Wu, J. Zhao, H. Wang, R. Guo, J. Xiao, B. Zhang, P. Yang, S. J. Pennycook, N. Deng, X. Yan and J. Chen, *Adv Funct Mater*, 2018, **28**, 1–10.

19 T. Song, R. Solanas, M. Qian, I. Fina and F. Sánchez, *J Mater Chem C Mater*, 2022, **10**, 1084–1089.

20 R. Takahashi, T. Yamamoto and M. Lippmaa, *Cryst Growth Des*, 2021, **21**, 5017–5026.

21 M. Mirjolet, F. Sánchez and J. Fontcuberta, *Adv Funct Mater*, 2019, **29**, 1808432.

22 S. Amoruso, A. Sambri and X. Wang, *J Appl Phys*, 2006, **100**, 013302.

23 A. Ojeda-G-P, M. Döbeli and T. Lippert, *Adv Mater Interfaces*, 2018, **5**, 1701062.

24 H. N. Lee, S. S. Ambrose Seo, W. S. Choi and C. M. Rouleau, *Sci Rep*, 2016, **6**, 19941.

25 J. V. Barth, G. Costantini and K. Kern, *Nature*, 2005, **437**, 671–679.

26 J. Lyu, I. Fina, R. Solanas, J. Fontcuberta and F. Sánchez, *Sci Rep*, 2018, **8**, 495.

27 P. Jiang, Q. Luo, X. Xu, T. Gong, P. Yuan, Y. Wang, Z. Gao, W. Wei, L. Tai and H. Lv, *Adv Electron Mater*, 2021, **7**, 2000728.

28 J. P. B. Silva, K. C. Sekhar, R. F. Negrea, J. L. MacManus-Driscoll and L. Pintilie, *Appl Mater Today*, 2022, **26**, 101394.

29 F. Cüppers, K. Hirai and H. Funakubo, *Nano Converg*, 2022, 9, 56.

30 J. Lyu, I. Fina and F. Sánchez, *Appl Phys Lett*, 2020, **117**, 072901.

31 T. Song, S. Estandía, H. Tan, N. Dix, J. Gàzquez, I. Fina and F. Sánchez, *Adv Electron Mater*, 2021, **8**, 2100420.